Elemental Carbon Cages†

T. G. Schmalz,* W. A. Seitz,* D. J. Klein,* and G. E. Hite*

Contribution from the Theoretical Chemical Physics Group, Department of Marine Sciences, Texas A&M University at Galveston, Galveston, Texas 77553. *Received April 2, 1987. Revised Manuscript Received September 23, 1987*

Abstract: Possible structures for stable carbon clusters of approximately 30–100 atoms are considered. On the basis of general chemical arguments, we establish several criteria for stable clusters which implicate hollow, three-dimensional cages with five- and six-membered rings. Approximate energy estimates indicate that cages should be the preferred cluster structure in this size regime. The effects of strain in the σ-bond system are argued to take a minimum value largely independent of cage size if the curvature of the cage is spread out isotropically. The relative stability of various cages thus depends dominantly on π-resonance energies which are computed by several semiempirical methods for a range of cages. All cages of up to 84 sites satisfying our major criteria are identified. All possible icosahedral-symmetry cages (which most strongly satisfy our criteria) are identified, with explicit consideration being given to those with up to 240 sites. In all we make explicit calculations on over 50 cages to check the efficacy of our criteria. Several theoretical conclusions are found to correlate with various molecular beam experiments, and a number of new candidates for especially stable structures are identified.

1. Introduction

Investigations of possible (kinetically) stable allotropic forms of elemental carbon most frequently focus on structures consisting of extended networks of covalent bonds. Besides the usual graphite and diamond forms, many structures have been considered.[1] Some experimental evidence[2] suggests still other forms whose structure is as yet incompletely determined.

A particularly interesting carbon structure was suggested recently by Kroto[3] et al. based upon the experimental observation of a stable C_{60} species formed by laser vaporization of graphite in a high-pressure supersonic nozzle.[3,4] They proposed that this species takes a "uniquely elegant" form corresponding to one of the Archimedean semiregular polyhedra, namely, a truncated icosahedron with carbon atoms at each of the vertices and σ-bonds along each edge. The resultant soccerball-like structure, dubbed[3] Buckminsterfullerene, and earlier[5-7] posited as a possible "superaromatic" species, is shown in Figure 1. For such a structure, π-like orbitals oriented normal to the surface are believed to make a resonance contribution to the stability of the system, as has indeed been indicated in several calculations.[6-21] Additional computations have also been done on other polyhedra: the regular dodecahedron,[6-8,11,15,17,18] the (semiregular) great rhombicosahedron,[12,17,18] the "graphitene" structure,[9,15,16] and a few others.[8,11,15-21] Moreover, Jones[22] has pointed out that larger such "hollow molecules" could yield condensed phases of anamolously low densities, and Zhang et al.[23] have proposed that similar cage-like structures may be involved in soot formation. Because of this widespread interest, a more systematic study of such clusters and associated criteria for greater (thermodynamic) stability is desirable, and we here embark upon such a study.

There is an enormous range of possible structures for clusters, not all of which are cages. In any case the most stable clusters should be those for which every carbon atom attains its tetravalency, preferably with little strain. While this might be done by a linear poly-yne chain[24] bent to close on itself to form a ring, reasonable limitation of the σ-strain implicates larger rings with little π-resonance energy per site due to bond alternation. Thus to achieve more significant resonance stabilization, we consider planar frameworks bent around upon themselves (in two directions) to form cages. Despite limiting the discussion in this way, we still face a very large number of possible isomeric species even for moderate-sized clusters. To guide the classification and to identify and focus on the most stable forms, we propose the following constraining criteria: (1) three-valent σ-network, (2) cage homeomorphic to a sphere, (3) five- and six-sided rings only, (4) higher symmetry, (5) no abutting five-sided rings, (6) curvature spread uniformly over the cage.

Some qualitative chemical rationale for criteria 1 to 5 are discussed in section 2, while criterion 6 is addressed in section 4. In the later sections where our calculations are reported, criteria 1 and 2 are presumed, while the remaining criteria are relaxed to varying degrees in order to test their importance in determining stability. Occasionally other researchers have invoked other

† Supported by the Robert A. Welch Foundation of Houston, Texas.

(1) See, e.g.: (a) Balaban, A. T.; Rentia, C. C.; Ciupitu, E. *Rev. Roum. Chim.* **1986**, *13*, 231. (b) Dias, J. R. *Carbon* **1984**, *22*, 107. (c) Hoffmann, R.; Hughbanks, T.; Kertesz, M.; Bird, P. H. *J. Am. Chem. Soc.* **1983**, *105*, 4831.

(2) See references in footnote 1 and also: (a) Whittaker, A. G. *Science* **1978**, *200*, 763. (b) Hayatsu, R.; Scott, G.; Studier, M. H.; Lewis, R. S.; Anders, E. *Ibid.* **1980**, *209*, 1515. (c) Donner, J. B. *Carbon* **1982**, *20*, 267.

(3) Kroto, H. W.; Heath, J. R.; O'Brien, S. C.; Curl, R. F.; Smalley, R. E. *Nature (London)* **1985**, *368*, 6042.

(4) Liu, Y.; O'Brien, S. C.; Zhang, Q. L.; Heath, J. R.; Tittel, F. K.; Curl, R. F.; Kroto, H. W.; Smalley, R. E. *Chem. Phys. Lett.* **1986**, *126*, 215.

(5) Yoshida, Z.; Osawa, E. In section 5.6.2 of *Aromatic Compounds* (in Japanese) (Kagakudojin, Kyoto, 1971).

(6) Bochvar, D. A.; Galipern, E. G. *Dokl. Akad. Nauk SSSR* **1973**, *209*, 610-612.

(7) Davidson, R. A. *Theor. Chim. Acta* **1981**, *58*, 193.

(8) Stankevich, I. V.; Nikerov, M. V.; Bochvar, D. A. *Usp. Khim.* **1984**, *53*, 1101 (Engl. trans.; *Russ. Chem. Rev.* **1984**, *53*, 640J).

(9) Haymet, A. D. J. *J. Am. Chem. Soc.* **1986**, *108*, 319.

(10) Klein, D. J.; Schmalz, T. G.; Seitz, W. A.; Hite, G. E. *J. Am. Chem. Soc.* **1986**, *108*, 1301.

(11) Hosoya, H. *Comp. Math. Appls.* **1986**, *12B*, 271.

(12) Haymet, A. D. J. *Chem. Phys. Lett.* **1985**, *122*, 421.

(13) Haddon, R. C.; Brus, L. E.; Raghavachari, K. *Chem. Phys. Lett.* **1986**, *125*, 459.

(14) Disch, R. L.; Schulman, J. M. *Chem. Phys. Lett.* **1986**, *125*, 465.

(15) Newton, M. D.; Stanton, R. E. *J. Am. Chem. Soc.* **1986**, *108*, 2469.

(16) Schmalz, T. G.; Seitz, W. A.; Klein, D. J.; Hite, G. E. *Chem. Phys. Lett.* **1986**, *130*, 203.

(17) Ozaki, M.; Takahashi, A. *Chem. Phys. Lett.* **1986**, *127*, 242.

(18) Fowler, P. W.; Woolrich, J. *Chem. Phys. Lett.* **1986**, *127*, 78.

(19) Klein, D. J.; Seitz, W. A.; Schmalz, T. G. *Nature (London)* **1986**, *323*, 705.

(20) Haddon, R. C.; Brus, L. E.; Raghavachari, K. *Chem. Phys. Lett.* **1986**, *131*, 165.

(21) The literature on this subject continues to grow rapidly. During the preparation of this manuscript we have become aware of the following additional publications: (a) Stone, A. J.; Wales, D. J. *Chem. Phys. Lett.* **1986**, *128*, 501. (b) Satpathy, S. *Ibid.* **1986**, *130*, 545. (c) Fowler, P. W. *Ibid.* **1986**, *131*, 444. (d) Marynick, D. S.; Estreicher, S. *Ibid.* **1986**, *132*, 383. (e) Harter, W. G.; Weeks, D. E. *Ibid.* **1986**, *21*, 387. (f) Nikolič, S.; Trinajstič, N. *Kem. Ind.* **1987**, *36*, 107.

(22) (a) Jones, D. E. H. *The Inventions of Daedalus*; W. H. Freeman: San Francisco, 1982; 3 pp 118, 119. (b) Jones, D. E. H. *New Sci.* **1966**, *32*, 245.

(23) Zhang, Q. L.; O'Brien, S. C.; Heath, J. R.; Liu, Y.; Curl, R. F.; Kroto, H. W.; Smalley, R. E. *J. Phys. Chem.* **1986**, *90*, 525.

(24) (a) Pitzer, K. S.; Clementi, E. *J. Am. Chem. Soc.* **1959**, *81*, 4477. (b) Strickler, S. J.; Pitzer, K. S. In *Molecular Orbitals in Chemistry, Physics and Biology*; Lowdin, P. O., Pullman, B., Ed.; Academic Press: New York, 1964; pp 281-291.

0002-7863/88/1510-1113$01.50/0

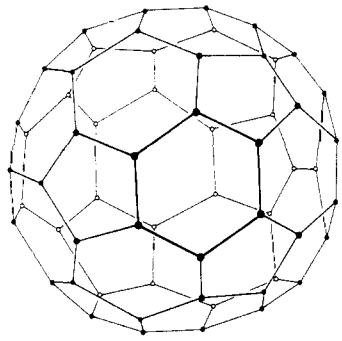

Figure 1. The "uniquely elegant" C_{60} structure proposed by Kroto et al.[3]

criteria, such as the restriction to regular or semiregular polyhedral cages, but we believe our criteria have a sounder chemical rationale. Section 3 identifies some first consequences of these various different criteria. Next, section 4 addresses questions concerning σ-strain in a general way, arguing that the ("isotropic" component of the) σ-strain is approximately proportional to a topological invariant that is the same for all cages which satisfy criterion 2. Further, support is found for criterion 6. Section 5 summarizes the arguments favoring our criteria. Empirical bond energy and force constant ideas are used to estimate nonresonant energies not only for cages, but also for several other types of clusters. For clusters with more than about 30 carbon atoms, cages appear as the best candidate for stable clusters.

As a consequence of the above arguments, the π-network energy emerges as the point of key focus differentiating the stabilities of different cages. Section 6 accounts for the diminution of the π-interaction due to the curvature of the π-network by introducing a single multiplicative correction to the π resonance energy. Section 7 describes the cages, more than 50 in number, that we select for study. In addition to various cages already considered in the literature, we systematically identify (as explained in the appendices) numerous others satisfying criteria 1 – 4. The focus is on "smaller" cages with fewer than about 80 vertices. Section 8 presents a critical discussion of the semiempirical schemes utilized to calculate π-resonance energy. Of these, our preferred approach is the so-called conjugated circuits method. In section 9 we briefly indicate our "transfer-matrix" technique for performing the requisite computations. Finally, sections 10 and 11 discuss the numerical results and their implications. Not only the Buckminsterfullerene C_{60} structure, but also several larger cages are identified as good candidates for especially stable species. Generally the calculations support our criteria.

2. Criteria for Carbon Clusters

As already mentioned, a one-dimensional (sp-hybridized) chain bent to close into a two-dimensional ring should exhibit little resonance energy. An sp^3-hybridized array of carbons would be three-dimensional and evidently either fill space (as does the diamond lattice) or have a surface with attendant (destabilizing) dangling bonds. Similarly an sp^2-hybridized planar fragment of the graphite lattice would have a reactive edge with dangling bonds. Thence we are led, at least for moderate-sized carbon clusters, to sp^2-hybridized networks bent around to close on themselves so that criterion 1 is preferred. To maximize stability there should be as little curvature as possible, for two reasons: first, so that the σ-skeleton achieves most nearly the ideal sp^2 geometry; and, second, so that the "overlap" between adjacent π-like orbitals is as large as possible. Hence if the σ-bonds are identified as edges of a polyhedron, the cages preferred are all homeomorphic to a sphere (that is, there are no doughnut holes as in a toroid), and criterion 2 is met.

Stability arguments suggest restrictions on ring sizes. As a general rule, π-electron stabilization is greatest for rings of size 6, somewhat less for sizes 5 and 7, and dramatically less for sizes 4 and 8. Rings of size 3 are rather unstable because of σ-strain, while rings of size ≥ 9 lead to generally diminishing π-resonance stabilization. Further, as we note in section 3, for each ring of size larger than 6 there must be "compensating" ring(s) of size less than 6, and there must be at least four (uncompensated) rings of size less than 6. Hence one anticipates that the most stable cages will have faces consisting of rings of size 5 or 6, as in criterion 3.

We propose to study only cages that exhibit a reasonable degree of symmetry. Because π-energetics (of stabilization) seem to be dominated by more or less local features, repetition of more stable local structures should yield the more stable global structures. Of course, the nature of Euclidean three-space places restrictions on the types of local structures and their interconnection. But repetition of local structures (including their interconnections) often results in symmetries, with symmetry operations rotating and/or reflecting the various local structures into one another, and criterion 4 is indicated.

Finally, the rationale for excluding fused five-membered rings is that when they abut there occurs an eight-cycle around the periphery of these two rings. But the (extended) Hückel $4n$-rule indicates this to be destabilizing, so that criterion 5 is motivated. A similar argument for three-membered rings suggests that they also are not very favorable since, in addition to introducing σ-strain, when one is abutted to an otherwise favorable hexagonal ring, there occurs an eight-cycle.

3. Consequences of the Criteria

In this section we will discuss a variety of consequences of the criteria of section 1 which restrict the classes of stable cage clusters. First there are some basic combinatoric relations. The restriction to three σ-bonds to each carbon site relates the number v of vertices and the number e of edges

$$2e = 3v \tag{3.1}$$

Similarly letting f_n denote the number of n-sided faces (or rings), one has

$$2e = \sum_n n f_n \tag{3.2}$$

A further condition on convex polyhedra is provided by Euler's theorem, which, when criterion 2 is satisfied, takes the form[25]

$$v + \sum_n f_n = e + 2 \tag{3.3}$$

From among the variables of these three equations one may eliminate any two. Thence elimination of e and v yields[25] a required balance between smaller and larger rings

$$3f_3 + 2f_4 + f_5 = 12 + \sum_n (n-6) f_n \tag{3.4}$$

If we work toward criterion 3 by choosing the only nonzero f_n to correspond to the more stable rings with $n = 5, 6, 7$, then

$$f_5 = 12 + f_7 \tag{3.5}$$

and

$$f_6 = v/2 - 10 - 2f_7 \tag{3.6}$$

While these conditions are necessary, they are not sufficient, in that there do not exist polyhedra for all possible sets of variables satisfying them. But it is known[26] that for any (nonnegative integer) choice of f_7 there do exist some values of f_6 for which a polyhedron is realizable. Moreover, in the important case that $f_7 = 0$ it is (constructively) known[26] that polyhedra are realizable for all f_6 other than 1. Beyond the rigorous results it appears that for many choices of the variables satisfying the above conditions there are still great numbers of different realizable polyhedra. Thus our additional symmetry criterion (4) plays an important role in giving us a more manageable list of potential systems to

(25) (a) Thompson, D'Arcy *Growth and Form*, 2nd ed.; Cambridge University Press: Cambridge, 1943; Chapter IX. (b) Smith, C. S. In *Metal Interfaces*; American Society of Metals: Cleveland, Ohio, 1952, Chapter 3. (c) Wells, A. F. *The Third Dimension in Chemistry*; Oxford University Press: London, 1956; Chapter 2. (d) Grunbaum, B. *Convex Polytopes*; Interscience: New York, 1967; Chapter 13.

(26) Grunbaum, B.; Motzkin, T. S. *Can. J. Math.* **1963**, *15*, 744.

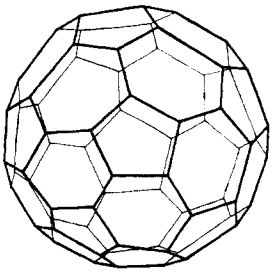

Figure 2. A C_{70} structure with no abutting five-membered rings.

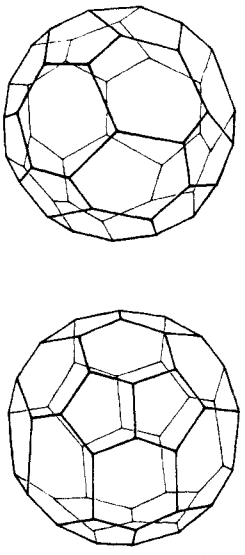

Figure 3. The two possible C_{50} structures with no five-membered ring adjacent to more than one other five-membered ring.

treat. Indeed upon restriction to the "highest" possible symmetry, namely icosahedral, the resulting polyhedra may be completely characterized: each such polyhedron uniquely corresponds to a pair of integers h, k such that $0 < h \geq k \geq 0$ with the number of vertices being

$$v = 20(h^2 + hk + k^2) \tag{3.7}$$

as is further discussed and proved in Appendix A. The "lower" symmetry cases seem to be not so well in hand but are further addressed in section 5.

Criterion 5, wherein fused five-membered rings are avoided, leads along with criteria 1, 2, and 3 to some interesting consequences. First, each of the 12 separate pentagonal faces has five distinct vertices, while any remaining vertices must be where three hexagonal faces join. Thence letting v' be the number of such vertices where three hexagons adjoin, we have

$$v = 60 + v' \tag{3.8}$$

Since v' is nonnegative, clearly $v \geq 60$. In fact the $v = 60$ Buckminsterfullerene structure of Figure 1 is the *unique* minimal polyhedron satisfying criteria 1–3 and 5, as shown in Appendix B. Upon making a diligent search for the next smallest such polyhedron, we suggest that the $v = 70$ structure of Figure 2 is unique in this regard. For $v < 60$, where criterion 5 cannot be realized, one might nevertheless seek to have a minimum of abutting pairs of five-membered rings.[27] Of course, there are fewer such pairs if five-sided rings do not adjoin in sets of three or more. The smallest cages satisfying this extended criterion turn out to be the two $v = 50$ cages of Figure 3 (as proved in Appendix C).

At this point we can already note some qualitative correlations with the available molecular-beam data on carbon clusters. First, for larger clusters only even numbers (v) of carbon atoms are observed[3,4,28-32] (at least at longer times), in agreement with (3.1).

(27) This idea was suggested by: Kroto, H. W., private communication.

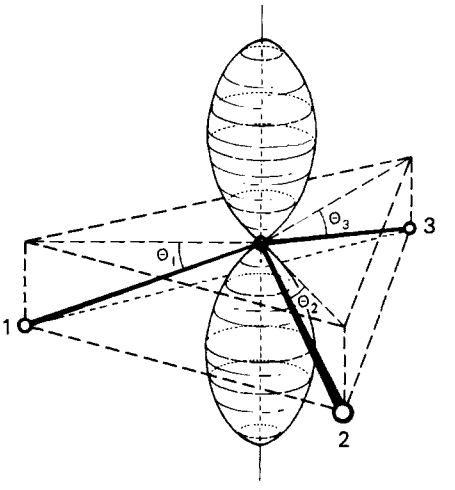

Figure 4. The alignment of a π-like orbital with regard to the nearest-neighbor sites 1, 2, 3.

Second, all even v are observed for $v \geq 24$, which, as we noted following (3.6), corresponds to allowed polyhedra. Third, there is some support for the notion that the experimentally observed clusters are cage-like in that the ionization potentials for the larger species are shifted from the ≈10-eV value[28] characteristic of poly-ynes to[33] the range 6.4–7.9 eV, somewhat nearer to the 3–4-eV values[28] characteristic of graphites. Fourth, the smallest (more entropically favored) cage satisfying criteria 1, 2, and 3 as well as either criterion 4, with the maximal icosahedral symmetry, or criterion 5, turns out to be the C_{60} Buckminsterfullerene structure proposed by Kroto et al.[3] Fifth, the next smallest cluster satisfying criteria 1, 2, 3, and 5, and incidentally having a relatively high symmetry (D_{5h}), appears to us to be the C_{70} structure of Figure 2, perhaps in correspondence with the next most abundant (long-time) mass-spectral peak observed.[3,4] Sixth, the smallest clusters (of Figure 3) satisfying criteria 1, 2, 3, and the extension of criterion 5 that no pentagon abuts to more than one other, are perhaps in correspondence with the third most abundant mass spectral peak (C_{50}) in the data from ref 3.

4. σ-Strain

Because the cage structures have "bent" surfaces, σ–π "separation" is not precise. But especially for the larger cages there should still be π-like orbitals oriented nearly normal to the surface and σ-like orbitals tangential to the surface. In that case there should be σ-bond strain due to imperfect alignment of bond-forming pairs of σ orbitals on adjacent carbon atoms and/or due to rehybridization of sp^2 orbitals to bring them into closer alignment. Likewise the π-like orbitals on neighboring carbon atoms do not align exactly parallel to one another, and the π interaction (as moderated by the resonance integral in Hückel theories or exchange integrals in valence-bond theories) should be diminished.

These matters are conveniently addressed in terms of the excess angles beyond a right angle of the angles between the π-orbital axis of a center and the straight-line directions to each of the three nearest neighbors. These three angles are identified by the label θ_i in Figure 4. For various reasonable choices of the direction of the π-like orbital, some of which are given in ref 10, 13, 18, 20, 34, and 35, these θ_i come out nearly equal, so that we denote

(28) Rohlfing, E. A.; Cox, D. M.; Kaldor, A. *J. Chem. Phys.* **1984**, *81*, 3322.
(29) Bloomfield, L. A.; Geusic, E. M.; Freeman, R. R.; Brown, W. L. *Chem. Phys. Lett.* **1985**, *121*, 33.
(30) Hahn, M. Y.; Honea, E. C.; Paguia, A. J.; Schriver, K. E.; Camarena, A. M.; Whetten, R. L. *Chem. Phys. Lett.* **1986**, *130*, 12.
(31) O'Keefe, A.; Ross, M. M.; Baronaski, A. P. *Chem. Phys. Lett.* **1986**, *130*, 17.
(32) Bernholc, J.; Phillips, J. C. *J. Chem. Phys.* **1986**, *85*, 3258.
(33) In a private communication the Rice University group has suggested this value is more nearly correct than the value of <5 eV in ref 28 (which, however, would make our argument even stronger).
(34) Haddon, R. C.; Scott, L. T. *Pure Appl. Chem.* **1986**, *58*, 137.

them by θ. (This θ is one-half that referred to in ref 10, 16, and 18.) Now a crucial mathematical point concerning these angles is that when their squares are summed over all vertices, the result is nearly constant

$$\sum\theta^2 \cong 4\pi/3\sqrt{3} \tag{4.1}$$

as indicated in Appendix D. This may be viewed as a type of "curvature conservation" statement to which there are corrections for "anisotropic" environments and for higher order terms in the power series expansion of bond angles in terms of θ.

With this "curvature conservation" result, a major point concerning the σ-strain may now be made. First, note that near-planar arrangements around a central vertex give rise to a σ-strain due to nonplanarity

$$\{\sigma\text{-strain at a vertex}\} \sim \tfrac{1}{2}k\theta^2 \tag{4.2}$$

with k a force constant. But combining this with (4.1), we obtain a total σ-strain due to nonplanarity

$$\{\text{net nonplanar } \sigma\text{-strain}\} \sim 2\pi k/3\sqrt{3} \tag{4.3}$$

That is, to within the approximation indicated here and in Appendix D, the σ-strain is independent of the cage.

An important qualification is clarified if we first note that the present result is equivalent to saying that the total amount of surface curvature needed to bend a planar structure into a (simple) closed surface is fixed. For the case of smooth surfaces this is a celebrated result from differential geometry,[36] where the surface's curvature (at a point) is defined to be the product of the curvatures[36] K_1 and K_2 along two orthogonal directions chosen so as to give the maximum result. In the case of isotropic curvature at a point, these curvatures are equal and the energy involved in (a slight) bending would be $\approx K_1K_2$. More generally for the anisotropic case the energy would be $\approx(K_1^2 + K_2^2)/2$. But clearly

$$(K_1^2 + K_2^2)/2 > K_1K_2 \tag{4.4}$$

so that corrections due to anisotropic curvature only add to (4.3). Thence the fusion of rings of rather differing sizes should be disfavored. Moreover, repulsive θ^4 corrections and bond-angle bending corrections as occur for smaller rings should add also, especially for the anisotropic case. As a consequence, three- and four-membered rings are disfavored, and we have motivated the isotropic cage criterion 6. The remaining π-electron energy contribution to the total energy tends also to give maximum stabilization for more isotropic structures, so that in seeking the most stable structures we need not presently quantify the anisotropic corrections to the σ-strain energy.

5. Nonresonant Cluster Energies

In combination with some simple bond-energy ideas our arguments from the preceding sections may be summarized in Figure 5. Data for the previously discussed general forms for carbon structures including chains, rings, graphite fragments, diamond-lattice fragments, and tori are given. These rough nonresonant energy estimates for a cluster of v sites, which exclude any contribution of π-electron resonance to the total energy, are referenced against v times the energy ϵ_g per site of an infinite graphite sheet. Of course, even the more compact finite fragments from such a sheet have edges with dangling bonds and as a consequence such v-site fragments have an energy greater than $v\epsilon_g$. The details of these rather approximate calculations are addressed in Appendix E. "Nonclassical" distortions of structures with dangling bonds could lead to corrections, presumably small, as for[37] C_6. The tori (or doughnut-shaped clusters) are estimated to have an isotropic curvature contribution twice that of cages. This is again readily seen from the viewpoint of differential geometry,[36] where it is

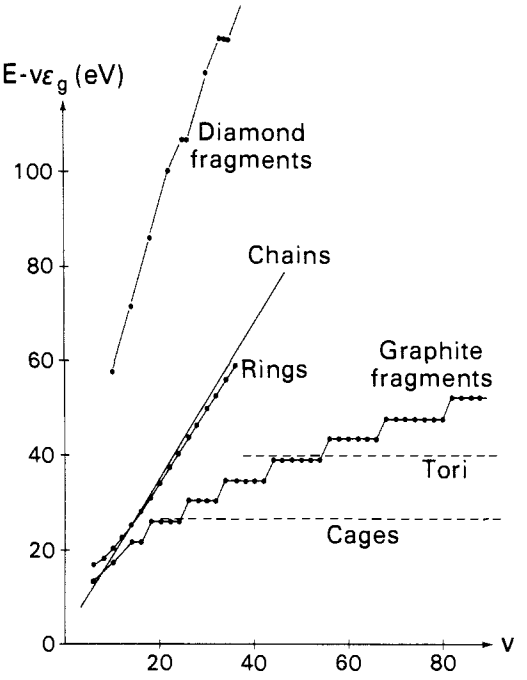

Figure 5. Nonresonant energy estimates for a variety of different types of carbon clusters.

well-known that for tori the Gaussian curvature K_1K_2 sums to zero, with K_1K_2 being positive on one-half of the surface and negative on the other half; since the minimum positive portion evidently is that for a polyhedron, and since what is of physical relevance is the absolute value $|K_1K_2|$, we obtain a total isotropic absolute-value curvature twice that for the polyhedra.

Despite the approximate nature of the estimates in Figure 5, several important qualitative conclusions are obtained. First the chains are preferred only for quite small v. Following this graphite fragments should be preferred up to $v \cong 24$. Then following this, cages should be preferred up to at least $v = 100$. For very large clusters there is some question whether there might be regions of anisotropic curvature away from the five-membered rings of these clusters, so that there might arise important corrections to the straight extension of the cage curve. But this is not certain and the possibility emerges that for all even $v > 30$ the cage structures give the thermodynamically preferred allotropic form of carbon. At least for the range ($30 \leq v < 100$) of focus in recent molecular beam experiments, isotropic cages are preferred, and this should remain true for somewhat larger v. As discussed in the last section, for cages of anisotropic shape or with small rings there should be additional (destabilizing) contributions. For perhaps $v \geq 60$ the toroidal clusters provide the second most stable family, though here there should always be some additional destabilization due to the anisotropy of curvature. In addition to comparisons at a fixed carbon number v, Figure 5 also allows an estimate of the size of a graphite fragment that would have the same (nonresonant) energy per site as a given cage. A rough calculation shows that fragments would have to be larger than about 160 carbon atoms to be more stable per site than a 60-atom cage, and larger than about 1400 carbon atoms to be more stable than a 180-atom cage. Of course, for these conclusions to be strictly valid, the resonance energy corrections for these different families should be comparable, as indeed we find in the following sections (at least when the more favored of the cages are considered).

6. π-Interaction Diminution

The discussion of curvature conservation in previous sections also has implications for the π-interaction diminution. This results from the misalignment of two π-like orbitals on neighboring sites, as indicated in Figure 4, where the θ values at the two neighbor sites are for convenience taken to be of equal magnitude (but rotated in opposite directions). Within Hückel-theoretic formu-

(35) (a) Haddon, R. C. *Chem. Phys. Lett.* **1986**, *125*, 1986. (b) Haddon, R. C. *J. Am. Chem. Soc.* **1986**, *108*, 2837. (c) Haddon, R. C. *Ibid.* **1987**, *109*, 1676. (d) Haddon, R. C. *J. Phys. Chem.* **1987**, *91*, 3719.

(36) See, e.g.: do Carmo, M. P. *Differential Geometry of Curves and Surfaces*; Prentice-Hall: Englewood Cliffs, New Jersey, 1976.

(37) Raghavachari, K.; Whiteside, R. A.; Pople, J. A. *J. Chem. Phys.* **1986**, *85*, 6623.

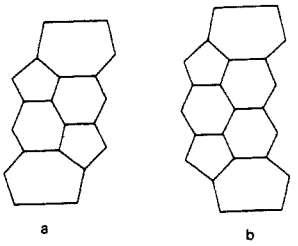

Figure 6. Choices for (unit) cells (composed of full rings) for the C_{60} and C_{70} structures of Figures 1 and 2.

lations the resultant resonance integral β_θ differs from β_0 for the planar case by a factor[10,13,18,20]

$$\{\pi\text{-interaction diminution factor}\} \sim 1 - c\theta^2 \qquad (6.1)$$

where c is positive and of order unity. The π interaction in valence-bond or resonance theories should likewise lead to such a diminution factor. Averaging (6.1) over all vertices and using (4.1), we then obtain

$$\{\text{average } \pi\text{-interaction diminution factor}\} \sim 1 - \frac{4\pi c}{3\sqrt{3}}\frac{1}{v} \qquad (6.2)$$

where we recall that v is the number of vertices. This argument says that a typical simple semiempirical π-electron calculation for a planar network is to be modified for the cage structures to within a first approximation just by multiplying the resultant π-interaction energy by the factor of (6.2). Multiplication of (6.2) onto a π-resonance energy scaling (size-extensively) as v, then gives a shift to the π-resonance energy which is independent of the number of carbon atoms. Of course, though v-independent, this correction term (just a fraction of the uncorrected π-resonance energy per site) should be strongly structure dependent.

The result, of (6.2), requires that the deviation away from the sp^2-hybridization ideal be small. Should the deviations be large as for the few cages considered with three- or four-membered rings, then there is additional strain and more π-interaction diminution. For the cages composed solely of five-, six-, and seven-membered rings, numerical tests reveal that the basic relation (4.1) is satisfied to within 5%, for reasonable choices of the θ angles of section 4.

7. Cages To Be Studied

As discussed in section 2 we focus primarily on polyhedral cages with some degree of symmetry. In particular we seek to identify all "smaller" cages satisfying criteria 1, 2, 3, and 4 such that the cage's symmetry group has an order greater than 12. Thence the symmetry groups we consider are those with n-fold rotational axes with $n \geq 4$, as well as the tetrahedral, octahedral, and icosahedral groups. First it is evident the n-fold rotation axes with $n = 4$ or $n \geq 7$ cannot occur with the criteria 1 and 3, since then there are no n-valent vertices or n-sided rings as would necessarily occur for such symmetries. This also precludes octahedral symmetries. Some few exceptions to these "forbidden" symmetries come when we relax criterion 3 to allow other rings (and thereby check the relevance of various criteria).

The cage structures are conveniently viewed as being built up through fusion of several symmetry-equivalent fragments or *cells*. That is, if such a cell is iterated via a symmetry group of operations, the whole surface (area) of the polyhedron is to be exactly covered. The idea here parallels that of crystallographic unit cells which generate the whole lattice when one cell is iterated via translations. Primitive cells corresponding to the polyhedra of Figures 1 and 2 are shown in Figure 6. That is, one obtains the structures of Figures 1 or 2 when gluing together five copies of either one of the cells in a cyclic fashion, say on the surface of a sphere, so that each cell adjoins on its boundaries to two others, "fore and aft". The manner in which we searched for the requisite cells having five- and six-fold symmetries and up to 88 sites is outlined in Appendix F. The resultant cells, other than those of Figure 6, are shown in Figure 7. An attempt at a similar search for cells of tetrahedral symmetries T_d or T_h was made, and we found the cells for polyhedra of up to 84 sites as in Figure 8. Here the primitive triangular-shaped cells are such that four copies glued together on the surface of a rounded tetrahedron yield the associated polyhedron. The icosahedral-symmetry case is considered in Appendix A and elsewhere.[19] The regular and semiregular polyhedra have all been extensively discussed in the general literature, dating back to Plato and Archimedes. Finally an example of a low-symmetry polyhedron satisfying the other criteria was considered, as a test of the symmetry criterion 4. Satisfying criterion 5 while avoiding criterion 4 requires a moderately large cage. The cage of C_{2v} symmetry we examine has 84 vertices, as shown in Figure 9.

The various polyhedra treated here are listed along with several of their structural characteristics in Table I. In this table a notation is utilized wherein a vertex joining three faces of i, j, and k sides is denoted by (i,j,k) and the number of such vertices is indicated by appending this number as an exponent to the symbol (i,j,k). Likewise the notation $(i,j)^m$ indicates there are m edges as interfaces between i- and j-sided faces. Finally $(i)^n$ indicates there are n faces with i sides.

8. π-Electron Resonance-Energy Schemes

As indicated in section 4, convex (isotropically curved) cages should be similarly affected by σ-strain. As a consequence we expect that the dominant effect serving to stabilize one cage

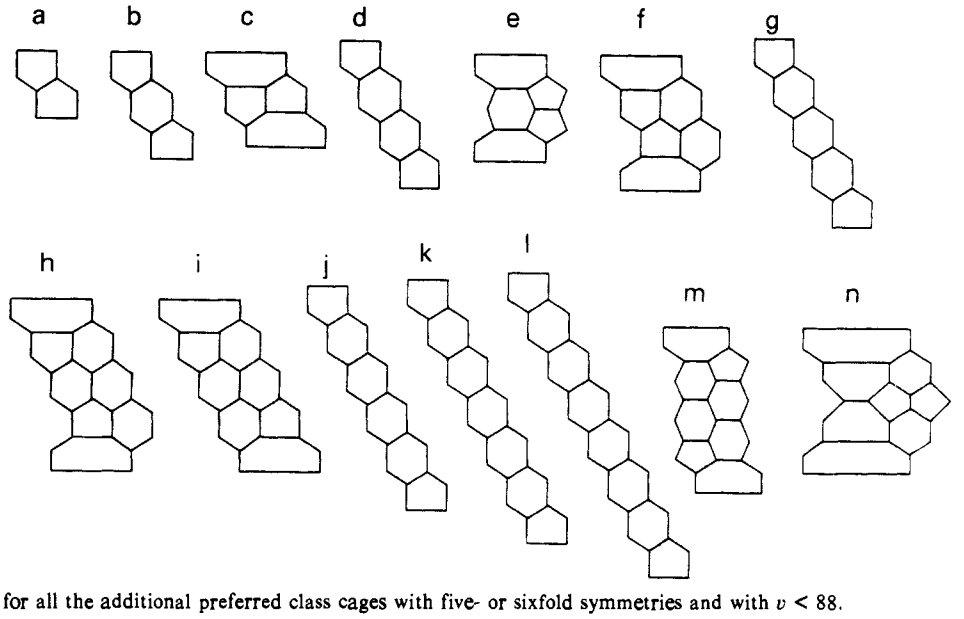

Figure 7. Basic cells for all the additional preferred class cages with five- or sixfold symmetries and with $v < 88$.

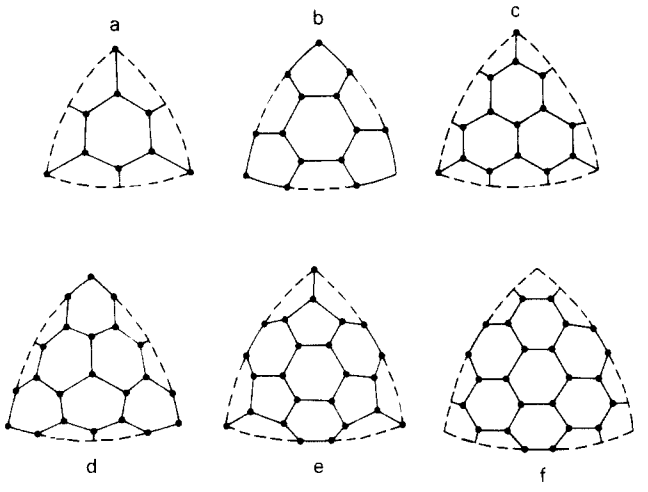

Figure 8. Basic cells for cages with tetrahedral symmetry T_d and $v < 88$.

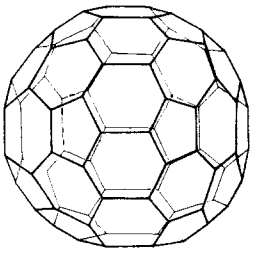

Figure 9. A $v = 84$ lower symmetry (C_{2v}) cage with no pairs of abutting pentagonal faces.

molecule relative to another is *π-electron resonance*. Thence we are able to apply several semiempirical computational schemes for the range of molecules of section 7.

The first group of calculations derives from Hückel molecular orbital (HMO) theory. The resultant total π-electron energy is then differenced against a reference energy to obtain the resonance energy. One traditional reference has been a sum over 2β for each double bond, where β is the HMO resonance integral. This is the first calculation reported in section 10.

The above method is not always reliable. For example, such calculations predict substantial stability for fused five-membered ring systems which is not found experimentally, and so application to cage molecules containing, of necessity, other than six-membered rings, is suspect. A method to focus on the extra stability conferred by delocalization in aromatic systems, regardless of ring size, was introduced by Hess and Schaad.[38] They suggested using a reference energy designed to predict exactly the HMO energy of acyclic conjugated hydrocarbons. This reference energy was written as an expansion over the types of bonds occurring in conjugated systems, and the expansion coefficients were determined by a least-squares fit to a data set of acyclic molecules. For carbon cage molecules, only two types of bonds occur (assuming all bonds to be the same length), and always in the same ratio, so the Hess and Schaad formula for resonance energy (RE) reduces to

$$\mathrm{RE} = E^{\pi} - Av\beta \tag{8.1}$$

where (as derived from ref 38) the constant $A = 1.5216$.

More recently, Jiang, Tang, and Hoffmann[39] have suggested an alternative form for the reference energy expression which depends on fewer parameters than the Hess and Schaad method. For carbon cages this alternative also reduces to the form of (8.1) but with a value of $A = 1.5332$. Although apparently not much different from the Hess and Schaad value, this value of A leads to a somewhat different view of the stability of carbon cages owing to the fact that A enters into a small difference between two large numbers in (8.1). We have recently examined the choice of a reference energy for Hückel theory using graph-theoretic cluster expansion.[40] This leads to unique solutions via inversion. Our conclusion is that the differences between the published results of Hess and Schaad and of Jiang, Tang, and Hoffmann are due primarily to biases in the data sets used in their least-squares fits rather than to "important" differences in the methods. We therefore suggest that (8.1) is indeed appropriate, but that the most reasonable value for A is about 1.507. This calculation is the second result reported in section 10.

The second group of calculations which we present starts with a consideration of the Kekulé structures of the molecules. For benzenoid systems the π-resonance energy is found to be simply proportional to the logarithm of the number of Kekulé structures.[41] We have therefore counted the Kekulé structures for all molecules considered via a method described more fully in the next section, and this count forms the basis of the third result in section 10.

It is well known that counting Kekulé structures does not adequately measure resonance in nonbenzenoid systems. Sometimes this can be remedied by using a corrected structure count[42] which involves a parity assignment to Kekulé structures. However, for cage molecules such as Buckminsterfullerene, it can be proved that it is not possible to assign a definite parity to a Kekulé structure. Still it is possible to improve upon the raw Kekulé count by examining the contribution of each Kekulé state to the *conjugated circuits* of the molecule. (By a conjugated circuit of length $2m$ we mean a cycle of $2m$ edges alternating between single and double bonds within a Kekulé structure.) Herndon's[43] quantitative resonance theory, equivalent to Randić's[44] conjugated circuit method, gives the π-resonance energy as a ratio H/K with

$$H = \sum_n \{R_n \#^{(4n+2)} + Q_n \#^{(4n)}\} \tag{8.2}$$

where K is the number of Kekulé structures, R_n and Q_n are oppositely signed parameters which decrease in magnitude near geometrically with increasing n, and where $\#^{(2m)}$ is the sum over the number of conjugated $2m$ circuits in the various Kekulé structures. Here again, ref 43 and 44 report slightly different parameter sets, but since no differences between large numbers are involved, both sets predict substantially the same results. We have chosen to use Herndon's parameters since we have truncated (8.2) at $n = 2$ while Randić's parameters assume truncation at $n = 3$ or 4. This calculation gives the fourth result of section 10.

9. Computational Methodology

Of the various computer calculations made, the most standard were those for the Hückel model. Matrix diagonalization was carried out, with the aid of block diagonalization due to the (cyclic) symmetries associated to the primitive cells.

The enumeration of Kekulé structures was carried out via a transfer matrix technique which has previously been described[45] in a more general context. In this approach the decomposition into cyclic-symmetry-equivalent cells plays a key role. For the purposes of this section the cells are chosen so that their boundaries bisect σ bonds. For M bisected σ bonds at a boundary shared with one of the two adjacent cells, the various possible patterns of π-bond occupancy in a Kekulé structure are denoted

$$\vec{\sigma} \equiv (\sigma_1, \sigma_2, \ldots, \sigma_M) \tag{9.1}$$

(38) Hess, B. A., Jr.; Schaad, L. J. *J. Am. Chem. Soc.* **1971**, *93*, 305.
(39) Jiang, Y.; Tang, A.; Hoffmann, R. *Theor. Chim. Acta* **1983**, *66*, 183.
(40) Schmalz, T. G.; Živković, T. P.; Klein, D. J. *Math/Chem/Comp* **1987**, Lacher, R. C., Ed.; Elsevier: New York, in press.
(41) Carter, P. G. *Trans. Faraday Soc.* **1949**, *45*, 597. (b) Swinbourne-Scheldrake, R.; Herndon, W. C.; Gutman, I. *Tetrahedron Lett.* **1975**, 755. (c) Seitz, W. A.; Klein, D. J.; Schmalz, T. G.; García-Bach, M. A. *Chem. Phys. Lett.* **1985**, *115*, 139; erratum, *Ibid.* **1985**, *118*, 110.
(42) (a) Wilcox, C. F., Jr. *Tetrahedron Lett.* **1968**, 795. (b) Trinajstić, N. *Chemical Graph Theory*, CRC Press: Boca Raton, FL, 1983; Vol. II.
(43) (a) Herndon, W. C. *J. Am. Chem. Soc.* **1973**, *95*, 2404. (b) Herndon, W. C.; Ellzey, M. L., Jr. *J. Am. Chem. Soc.* **1974**, *96*, 6631.
(44) (a) Randić, M. *Tetrahedron* **1975**, *31*, 1477. (b) Randić, M.; Trinajstić, N. *J. Am. Chem. Soc.* **1984**, *106*, 4428.
(45) Klein, D. J.; Hite, G. E.; Schmalz, T. G. *J. Comput. Chem.* **1986**, *7*, 443.

Table I

sequence no.	vertices	edges	faces	overall symmetry	unit cells	figure	description
1	$(3^3)^4$	$(3,3)^6$	$(3)^4$	T_d	$(3)^4$		regular tetrahedron
2	$(4^3)^8$	$(4,4)^{12}$	$(4)^6$	O_h			cube
3	$(4^2,6)^{12}$	$(4^2)^6(4,6)^{12}$	$(4)^6(6)^2$	D_{6h}	$(4)^6$		hexagonal prism
4	$(3,6^2)^{12}$	$(3,6)^{12}(6^2)^6$	$(3)^4(6)^4$	T_d	$(6,3)^4$		truncated tetrahedron
5	$(4^2,8)^{16}$	$(4^2)^8(4,8)^{16}$	$(4)^8(8)^2$	D_{8h}	$(4)^8$		octagonal prism
6	$(4^2,10)^{20}$	$(4^2)^{10}(4,10)^{20}$	$(4)^{10}(10)^2$	D_{10h}	$(4)^{10}$		decagonal prism
7	$(5^3)^{20}$	$(5^2)^{30}$	$(5)^{12}$	I_h	$(5,5)^5$	7a	regular dodecahedron
8	$(5^2,6)^{12}(5^3)^{12}$	$(5^2)^{24}(5,6)^{12}$	$(5)^{12}(6)^2$	D_{6d}	$(5,5)^6$	7a	
9	$(4,6^2)^{24}$	$(4,6)^{24}(6^2)^{12}$	$(4)^6(6)^8$	O_h			truncated octahedron
10	$(3,8^2)^{24}$	$(3,8)^{24}(8^2)^{12}$	$(3)^8(8)^6$	O_h			truncated cube
11	$(5^3)^4(5^2,6)^{24}$	$(5^2)^{18}(5,6)^{24}$	$(5)^{12}(6)^4$	T_d	$(6,5^3)^4$	8a	
12	$(5^2,7)^{14}(5^3)^{14}$	$(5^2)^{28}(5,7)^{14}$	$(5)^{14}(7)^2$	D_{7d}	$(5,5)^7$	7a	
13	$(5^3)^{10}(5^2,6)^{10}(5,6^2)^{10}$	$(5^2)^{20}(5,6)^{20}(6^2)^5$	$(5)^{12}(6)^5$	D_{5h}	$(5^2,6)^5$	7b	
14	$(5^2,6)^{24}(5,6^2)^{12}$	$(5^2)^{12},(5,6)^{36}(6^2)^6$	$(5)^{12}(6)^8$	D_{6h}	$(5^26)^6$	7b	
15	$(5^2,6)^{20}(6^2,5)^{20}$	$(5^2)^{10}(5,6)^{40}(6^2)^{10}$	$(5)^{12}(6)^{10}$	D_{5d}	$(5^2,6^2)^5$	7c	
16	$(5^3)^{10}(5^2,6)^{10}(5,6^2)^{10}(6^3)^{10}$	$(5^2)^{20}(5,6)^{20}(6^2)^{20}$	$(5)^{12}(6)^{10}$	D_{5d}	$(5^2,6^2)^5$	7d	
17	$(5^3)^4(5^2,6)^{12}(5,6^2)^{24}$	$(5^2)^{12}(5,6)^{36}(6^2)^{12}$	$(5)^{12}(6)^{10}$	T_d	$(5^3,6^{5/2})^4$	8b	
18	$(5^2,6)^{14}(5^2,7)^{14}(5,6^2)^{14}$	$(5^2)^{14}(5,6)^{28}(5,7)^{14}(6^2)^7$	$(5)^{14}(6)^7(7)^2$	D_{7h}	$(5^2,6)^7$	7b	
19	$(5^2,6)^{24}(5,6^2)^{12}(6^3)^{12}$	$(5^2)^{12}(5,6)^{36}(6^2)^{24}$	$(5)^{12}(6)^{14}$	D_{6d}	$(5^2,6^2)^6$	7c	
20	$(5^2,6)^{24}(5,6^2)^{12}(6^3)^{12}$	$(5^2)^{12}(5,6)^{36}(6^2)^{24}$	$(5)^{12}(6)^{14}$	D_{6d}	$(5^2,6^2)^6$	7d	
21	$(4,6,8)^{48}$	$(4,6)^{24}(4,8)^{24}(6,8)^{24}$	$(4)^{12}(6)^8(8)^6$	O_h			truncated cuboctahedron
22	$(5^2,6)^{12}(5,6^2)^{36}(6^3)^2$	$(5^2)^6(5,6)^{48}(6^2)^{21}$	$(5)^{12}(6)^{15}$	D_3	$(5^4,6^5)^3$	3b	
23	$(5^3)^{10}(5^2,6)^{10}(5,6^2)^{10}(6^3)^{20}$	$(5^2)^{20}(5,6)^{20}(6^2)^{35}$	$(5)^{12}(6)^{15}$	D_{5h}	$(5^2,6^3)^5$	7g	
24	$(5^2,6)^{10}(5,6^2)^{40}$	$(5^2)^5(5,6)^{50}(6^2)^{20}$	$(5)^{12}(6)^{15}$	D_{5h}	$(5^2,6^3)^5$	3a, 7e	
25	$(5^3)^4(5^2,6)^{12}(5,6^2)^{24}(6^3)^{16}$	$(5^2)^{12}(5,6)^{36}(6^2)^{36}$	$(5)^{12}(6)^{18}$	T_d	$(5^3,6^{9/2})^4$	8c	
26	$(5^2,6)^{14}(5^2,7)^{14}(5,6^2)^{14}(6^3)^{14}$	$(5^2)^{14}(5,6)^{28}(5,7)^{14}(6^2)^{28}$	$(5)^{14}(6)^{14}(7)^2$	D_{7d}	$(5^2,6^2)^7$	7d	
27	$(5^2,6)^{10}(5,6^2)^{40}(6^3)^{10}$	$(5^2)^5(5,6)^{50}(6^2)^{35}$	$(5)^{12}(6)^{20}$	D_5	$(5^2,6^4)^5$	7f	
28	$(5^3)^{10}(5^2,6)^{10}(5,6^2)^{10}(6^3)^{30}$	$(5^2)^{20}(5,6)^{20}(6^2)^{50}$	$(5)^{12}(6)^{20}$	D_{5d}	$(5^2,6^4)^5$	7j	
29	$(5^2,6)^{24}(5,6^2)^{12}(6^3)^{24}$	$(5^2)^{12}(5,6)^{36}(6^2)^{42}$	$(5)^{12}(6)^{20}$	D_{6h}	$(5^2,6^3)^6$	7g	
30	$(5^2,6)^{12}(5,6^2)^{36}(6^3)^{12}$	$(5^2)^6(5,6)^{48}(6^2)^{36}$	$(5)^{12}(6)^{20}$	D_{6h}	$(5^2,6^3)^6$	7e	
31	$(3,10^2)^{60}$	$(3,10)^{60}(10^2)^{30}$	$(3)^{20}(10)^{12}$	I_h			truncated dodecahedron
32	$(5,6^2)^{60}$	$(5,6)^{60}(6^2)^{30}$	$(5)^{12}(6)^{20}$	I_h	$(5^2,6^4)^5$	1, 6a	truncated icosahedron
33	$(5^2,6)^{12}(5,6^2)^{36}(6^3)^{20}$	$(5^2)^6(5,6)^{48}(6^2)^{48}$	$(5)^{12}(6)^{24}$	T_d	$(5^3,6^6)^4$	8d	
34	$(5^2,6)^{14}(5^2,7)^{14}(5,6^2)^{14}(6^3)^{28}$	$(5^2)^{14}(5,6)^{28}(5,7)^{14}(6^2)^{49}$	$(5)^{14}(6)^{21}(7)^2$	D_{7h}	$(5^2,6^3)^7$	7g	
35	$(5,6^2)^{60}(6^3)^{10}$	$(5,6)^{60}(6^2)^{45}$	$(5)^{12}(6)^{25}$	D_{5h}	$(5^2,6^5)^5$	2, 6b	
36	$(5^3)^{10}(5^2,6)^{10}(5,6^2)^{10}(6^3)^{40}$	$(5^2)^{20}(5,6)^{20}(6^2)^{65}$	$(5)^{12}(6)^{25}$	D_{5h}	$(5^2,6^5)^5$	7k	
37	$(5^2,6)^{12}(5,6^2)^{36}(6^3)^{24}$	$(5^2)^6(5,6)^{48}(6^2)^{54}$	$(5)^{12}(6)^{26}$	D_6	$(5^2,6^4)^6$	7f	
38	$(5^2,6)^{24}(5,6^2)^{12}(6^3)^{36}$	$(5^2)^{12}(5,6)^{36}(6^2)^{60}$	$(5)^{12}(6)^{26}$	D_{6d}	$(5^2,6^4)^6$	7j	
39	$(5,6^2)^{60}(6^3)^{12}$	$(5,6)^{60}(6^2)^{48}$	$(5)^{12}(6)^{26}$	D_{6d}	$(5^2,6^4)^6$	6a	
40	$(5,6^2)^{60}(6^3)^{16}$	$(5,6)^{60}(6^2)^{54}$	$(5)^{12}(6)^{28}$	T_d	$(5^3,6^7)^4$	8e	
41	$(5,6^2)^{60}(6^3)^{20}$	$(5,6)^{60}(6^2)^{60}$	$(5)^{12}(6)^{30}$	D_{5d}	$(5^2,6^6)^5$	7m	
42	$(5,6^2)^{60}(6^3)^{20}$	$(5,6)^{60}(6^2)^{60}$	$(5)^{12}(6)^{30}$	D_{5h}	$(5^2,6^6)^5$	7i	
43	$(5^2,6)^{10}(5,6^2)^{40}(6^3)^{30}$	$(5^2)^5(5,6)^{50}(6^2)^{65}$	$(5)^{12}(6)^{30}$	D_{5h}	$(5^2,6^6)^5$	7n	
44	$(5^3)^{10}(5^2,6)^{10}(5,6^2)^{10}(6^3)^{50}$	$(5^2)^{20}(5,6)^{20}(6^2)^{80}$	$(5)^{12}(6)^{30}$	D_{5d}	$(5^2,6^6)^5$	7l	
45	$(5,6^2)^{60}(6^3)^{20}$	$(5,6)^{60}(6^2)^{60}$	$(5)^{12}(6)^{30}$	I_h	$(5^2,6^6)^5$	7h	$h = 2, k = 0$, Appendix A
46	$(5,6^2)^{60}(6^3)^{24}$	$(5,6)^{60}(6^2)^{66}$	$(5)^{12}(6)^{32}$	C_{2v}		9	
47	$(5^2,6)^{24}(5,6^2)^{12}(6^3)^{48}$	$(5^2)^{12}(5,6)^{36}(6^2)^{78}$	$(5)^{12}(6)^{32}$	D_{6h}	$(5^2,6^5)^6$	7k	
48	$(5,6^2)^{60}(6^3)^{24}$	$(5,6)^{60}(6^2)^{66}$	$(5)^{12}(6)^{32}$	D_{6h}	$(5^2,6^5)^6$	6b	
49	$(5,6^2)^{60}(6^3)^{24}$	$(5,6)^{60}(6^2)^{66}$	$(5)^{12}(6)^{32}$	T_d	$(5^3,6^8)^4$	8f	
50	$(5^2,6)^{14}(5^2,7)^{14}(5,6^2)^{14}(6^3)^{42}$	$(5^2)^{14}(5,6)^{28}(5,7)^{14}(6^2)^{70}$	$(5)^{14}(6)^{28}(7)^2$	D_{7d}	$(5^2,6^4)^7$	7j	
51	$(4,6,10)^{120}$	$(4,6)^{60}(4,10)^{60}(6,10)^{60}$	$(4)^{30}(6)^{20}(10)^{12}$	I_h			truncated icosadodecahedron
52	$(5,6^2)^{60}(6^3)^{80}$	$(5,6)^{60}(6^2)^{150}$	$(5)^{12}(6)^{60}$	I			$h = 2, k = 1$, Appendix A
53	$(5,6^2)^{60}(6^3)^{120}$	$(5,6)^{60}(6^2)^{210}$	$(5)^{12}(6)^{80}$	I_h			$h = 3, k = 0$, Appendix A
54	$(5,6^2)^{60}(6^3)^{180}$	$(5,6)^{60}(6^2)^{300}$	$(5)^{12}(6)^{110}$	I_h			$h = k = 2$, Appendix A

where $\sigma_i = 0$ or 1 as the ith σ bond is unoccupied or occupied by a π bond also. Then we let $(\vec{\tau}|\mathrm{T}|\vec{\sigma})$ denote the number of different ways that "leading" and "trailing" boundaries of the cell can have the occupancy patterns $\vec{\tau}$ and $\vec{\sigma}$. The resultant *transfer matrix* nicely identifies the manners of propagation of Kekulé structures through a unit cell. An element of a power of T, say $(\vec{\tau}|\mathrm{T}^q|\vec{\sigma})$, identifies the number of different ways that the leading and trailing boundaries of a sequence of q cells can have the occupancy patterns $\vec{\tau}$ and $\vec{\sigma}$. With p cells connected in a cyclic pattern, the total number of Kekulé structures is then given by

$$K = \sum_{\vec{\sigma}} (\vec{\sigma}|\mathrm{T}^p|\vec{\sigma}) = \mathrm{tr}\mathrm{T}^p \qquad (9.2)$$

This method is quite efficient because of the simplicity of the individual matrix elements of T. In most of our cases their values were only 0, 1, or 2 with the vast majority being 0. E.g., for C_{240}, our T had more than 99% of its elements 0, so that sparse matrix techniques were used, as is fairly crucial for manipulating the overall 2^{11} by 2^{11} transfer matrix which arises in this case.

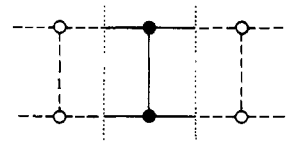

Figure 10. A basic cell for the transfer matrix for prisms. The two adjacent cells are indicated with dotted lines.

An example, for the (semiregular) p-sided prism, serves to illustrate the method. The basic cell is chosen as in Figure 10, where the two vertical dotted lines indicate the boundaries of the central cell. There are four possible occupancy patterns at a boundary:

$$(0,0),\ (1,1),\ (0,1),\ (1,0) \qquad (9.3)$$

Now, for example, if the left-hand boundary has occupancy patterns (0,0) then as indicated in Figure 11, the only two occupancy patterns that may follow it at the right-hand boundary

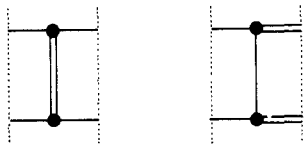

Figure 11. Diagrams for nonzero elements of the transfer matrix, as occur in the column labeled by (0,0).

are (0,0) and (1,1). Thus in the first column of T (with rows and columns ordered as in (9.3)) the only two nonzero elements (=1) are the first and second. The whole transfer matrix is

$$\mathbf{T} = \begin{pmatrix} 1 & 1 & 0 & 0 \\ 1 & 0 & 0 & 0 \\ 0 & 0 & 0 & 1 \\ 0 & 0 & 1 & 0 \end{pmatrix} \tag{9.4}$$

The blocking of T is, in fact, a general feature which may be utilized to simplify the calculation of (9.2). (For long polymer species such blocking has been associated with a long-range order with possible novel physical implications[46]). From (9.2) one sees that the Kekulē count K_p for a p-sided prism is just the sum of the pth powers of the eigenvalues of T in (8.4),

$$K_p = 1 + (-1)^p + \left(\frac{1+\sqrt{5}}{2}\right)^p + \left(\frac{1-\sqrt{5}}{2}\right)^p \tag{9.5}$$

Alternatively the sum of the last two powers here could be obtained as the pth member of the Fibonacci-like sequence 1, 3, 4, 7, 11, 18, 29, ...

The conjugated-circuit enumerations are carried out by a modification of the transfer matrix method which in addition to T also involves *connection matrices* $\mathbf{C}^{(\alpha)}$. These are defined with $(\vec{\tau}|\mathbf{C}^{(\alpha)}|\vec{\sigma})$ being the number of different ways that leading and trailing boundaries of a sequence of cells containing the circuit α can have the occupancy patterns $\vec{\tau}$ and $\vec{\sigma}$ at the same time conjugation occurs about α. Then

$$\#^{(2m)} = \sum_{\alpha}^{2m} \mathrm{tr}(\mathbf{C}^{(\alpha)}\mathbf{T}^q) \tag{9.6}$$

where the sum is over all circuits of size $2m$ and q counts the number of unit cells not accounted for in $\mathbf{C}^{(\alpha)}$. Often this sum can be much simplified because many of the circuits α are symmetry equivalent.

Again the p-sided prism serves to illustrate the approach. The conjugated circuits surrounding one or more lateral (four-sided) faces of such a prism may be dealt with in a general fashion, since the state (0,0) both precedes and succeeds any such circuit. Then the connection matrix for any such circuit is

$$\mathbf{C}^{(\alpha)} = \begin{pmatrix} 2 & 0 & 0 & 0 \\ 0 & 0 & 0 & 0 \\ 0 & 0 & 0 & 0 \\ 0 & 0 & 0 & 0 \end{pmatrix} \tag{9.7}$$

with $\alpha = p - m$ for a $2m$ circuit (spanning m unit cells). Thence since there are p possible choices for the positioning of such a conjugated circuit, we obtain

$$\#^{(2m)} = 2p(0,0|\mathbf{T}^{p-m}|0,0) + \text{cap corrections} \tag{9.8}$$

where the cap corrections involve conjugated circuits surrounding one (or both) of the prism's end faces. Again the expression in (9.8) may be written in terms of powers of eigenvalues of T.

$$\#^{(2m)} = 2p\left\{\frac{5+\sqrt{5}}{10}\left(\frac{1+\sqrt{5}}{2}\right)^{p-m} + \frac{5-\sqrt{5}}{10}\left(\frac{1-\sqrt{5}}{2}\right)^{p-m}\right\} + \text{cap corrections} \tag{9.9}$$

(46) See, e.g.: Klein, D. J.; Schmalz, T. G.; Seitz, W. A.; Hite, G. E. *Int. J. Quantum Chem.* **1986**, *19S*, 707.

Table II. Kekulē-Structure and Conjugated-Circuit Counts for the Polyhedra Investigated

sequence no.	v	K	$\#^{(4)}$	$\#^{(6)}$	$\#^{(8)}$	$\#^{(10)}$
1	4	3	6	0	0	0
2	8	9	24	24	12	0
3	12	20	60	54	60	48
4	12	8	0	8	30	12
5	16	49	208	128	88	80
6	20	125	880	420	260	168
7	20	36	0	0	240	120
8	24	54	0	16	336	96
9	24	169	600	320	672	744
10	24	32	0	0	192	144
11	28	75	0	48	144	0
12	28	113	0	0	784	364
13	30	151	0	180	740	300
14	36	272	0	368	624	156
15	40	562	0	1420	940	800
16	40	701	0	1720	3600	2300
17	40	576	0	1272	1800	648
18	42	673	0	952	1848	1750
19	48	1666	0	5984	2976	3960
20	48	1782	0	5344	4344	3528
21	48	16384	130560	35712	89484	90960
22	50	2136	0	7956	1920	5058
23	50	3376	0	12620	17800	15410
24	50	2343	0	9840	1800	6320
25	56	6561	0	28848	19656	27048
26	56	4901	0	14728	13076	19180
27	60	9183	0	40140	10720	28220
28	60	16501	0	83000	88500	96380
29	60	12740	0	60680	31824	46056
30	60	12688	0	65968	17016	46416
31	60	2048	0	0	0	768
32	60	12500	0	83160	0	59760
33	68	26244	0	129600	33696	94680
34	70	81251	0	513800	441000	577700
35	70	52168	0	389960	0	293630
36	70	38711	0	182476	101920	203840
37	72	66817	0	445568	64680	340572
38	72	93654	0	611680	236040	494016
39	72	77400	0	653784	0	497616
40	76	105600	0	760368	0	585480
41	80	214775	0	1676760	187460	1332170
42	80	169375	0	1169340	0	876560
43	80	401876	0	2511640	2200000	2619060
44	80	270153	0	2466320	0	1939840
45	80	140625	0	835800	0	644280
46	84	588380	0	4619328	0	3765206
47	84	694928	0	5761280	1757520	4815444
48	84	446032	0	4091200	0	3222684
49	84	499392	0	5053392	0	4508568
50	84	317864	0	2067240	828492	2126796

Alternatively the term in brackets may be identified as the $(p - m)$th member of the Fibonacci sequence 1, 2, 3, 5, 8, 13, 21, ... For $2m \leq 10$, the end corrections are nonzero only for $p = 4, 6, 8, 10$. They can be readily evaluated by similar methods.

The exact numerical counts resulting from the application of the transfer matrix to the polyhedral structures of Table I are reported in Table II. The results for the last four structures are given elsewhere[19] and are not reported here (since the exact counts of up to 18 digits do not so conveniently fit into the format of the present table). Evidently the Kekulē count (and associated conjugated-circuit counts when nonzero) increases roughly in an exponential fashion with v. Notably, of the half-dozen C_{60} cages three display more Kekulē structures than the Buckminsterfullerene structure.

10. Resonance Energies and Related Results

The numerical results of Table II may be utilized as indicated in section 8 to obtain two resonance-energy estimates. These, along with the two other Hückel-MO-related estimates indicated in section 8, then are reported in Table III. The resonance energies per site reported here are in units of the corresponding reso-

Table III. Resultant Data for Carbon Cages

sequence no.	per-site energy ratios to graphite: Kekulē count	conjugated circuit	Hückel delocalization	corrected Hückel	HOMO–LUMO gap (β)	criteria
1	1.700	−1.929	0.000	−7.500	0	(3)r
2	1.700	+0.121	0.870	−0.104	2.0000	(3)r
$v = 12$ 3	1.545	+0.172	0.580	−2.569	0	(3)s
$v = 12$ 4	1.073	+0.183	0.870	−0.104	1.0000	(3)s
5	1.506	−0.178	0.796	−0.738	0.8284	(3,6)s
20 6	1.495	−0.546	0.778	−0.884	0.7639	(3,6)s
20 7	1.109	−0.182	0.819	−0.535	0	(5)r
24 8	1.029	−0.191	0.828	−0.461	0	(5)
24 9	1.323	−0.067	0.863	−0.166	0.8284	(3)s
24 10	0.894	−0.019	0.824	−0.492	0	(3)s
28 11	0.955	−0.008	0.836	−0.394	0	(5)
28 12	1.045	−0.153	0.837	−0.389	0	(3?,5)
13	1.035	+0.078	0.863	−0.163	0	(5)
14	0.964	+0.121	0.890	+0.067	0	(5)
40 15	0.980	+0.322	0.919	+0.313	0.3731	(4?,5)
40 16	1.014	+0.272	0.888	+0.044	0	(5)
40 17	0.984	+0.211	0.897	+0.127	0	(5)
18	0.960	+0.191	0.895	+0.112	0	(3?,5)
48 19	0.957	+0.415	0.925	+0.365	0.2135	(4?,5)
48 20	0.965	+0.316	0.921	+0.332	0	(5)
48 21	1.252	−0.359	0.818	−0.551	0	(3)s
50 22	0.949	+0.439	0.942	+0.509	0.4680	(4,5)
50 23	1.006	+0.393	0.904	+0.188	0	(5,6)
50 24	0.961	+0.503	0.938	+0.475	0.1031	(5)
56 25	0.972	+0.456	0.930	+0.404	0.2316	(5)
56 26	0.939	+0.334	0.925	+0.365	0	(3?,5)
60 27	0.942	+0.436	0.931	+0.417	0	(4?,5)
60 28	1.002	+0.475	0.917	+0.295	0	(5,6)
60 29	0.975	+0.452	0.938	+0.475	0	(5,6?)
60 30	0.975	+0.520	0.943	+0.515	0.1031	(5)
60 31	0.787	+0.012	0.843	−0.331	0.5069	s
60 32	0.973	+0.712	0.962	+0.676	0.7566	(3)s
33	0.926	+0.439	0.936	+0.458	0	(5)
70 34	1.000	+0.534	0.927	+0.379	0	(5,6?)
70 35	0.961	+0.693	0.965	+0.702	0.5293	
70 36	0.934	+0.428	0.942	+0.503	0	(5,6)
72 37	0.955	+0.583	0.946	+0.539	0.0167	(5)
72 38	0.984	+0.545	0.949	+0.564	0	(5,6)
72 39	0.968	+0.764	0.969	+0.732	0.7023	
40	0.942	+0.618	0.954	+0.609	0	
80 41	0.950	+0.625	0.958	+0.640	0	(4?)
80 42	0.932	+0.560	0.953	+0.596	0	
80 43	0.999	+0.447	0.935	+0.449	0	(5)
80 44	0.968	+0.749	0.965	+0.706	0.0728	(5,6)
80 45	0.917	+0.485	0.946	+0.544	0	
84 46	0.979	+0.618	0.969	+0.735	0.3285	(4)
84 47	0.991	+0.611	0.956	+0.626	0	(5,6)
84 48	0.959	+0.717	0.968	+0.732	0.5293	
84 49	0.967	+0.816	0.972	+0.766	0.6962	
84 50	0.934	+0.497	0.952	+0.592	0	(5,6?)
51	1.228	−0.430	0.849	−0.280	0.3511	(3)s
52	0.951	+0.772	0.973	+0.769	0	
53	0.962	+0.984	0.987	+0.888	0.5795	
54	0.970	+0.923	0.990	+0.916	0.4964	

nance-energy estimates for graphite and are uncorrected for π-strain, i.e., are without the π-interaction diminution factor of section 6. The graphite Hückel-MO value of 0.57460β that we used improves slightly on that of Coulson and Rushbrooke.[47] The graphite Kekulē-structure-count value of $0.183J$ is obtained by numerical evaluation of a one-dimensional integral giving an exact result.[48] The conjugated-circuit value is not yet so precisely known, so that we used a resonance energy per site estimate of 0.1685 eV as obtained by extrapolation of (numerically) exact calculations for increasing-width infinitely long strips cut from the graphite lattice. As is seen from the table, the resonance energies per site of the larger more graphite-like structures (C_{180}, and C_{240}) approach those of graphite, as one might anticipate.

As noted in section 8 the conjugated-circuit result is believed to give the most reliable result. The Hückel delocalization energy is in poor agreement, though the more sophisticated Hückel-based approach (of Hess and Schaad[38] or Jiang, Tang, and Hoffmann[39] but with our parameterization[40]) is in semiquantitative agreement. Indeed the parameterization we use gives closer agreement than earlier ones evidently due to the fact that these earlier parameterizations emphasized agreement with structures with a lower "degree of branching" (rather unlike that for the current cages). The Kekulē-count result is also in poor agreement with the preferred conjugated-circuit result, though there is some rough correspondence between the Kekulē-count result and the Hückel delocalization energy.

Table III also reports two other relevant pieces of data. First there is the Hückel HOMO–LUMO gap, which when 0 or very small we feel is an indication of (open-shell) reactivity, and/or a propensity for Jahn–Teller distortion. Finally the last column of the table concerns various criteria which each cage satisfies.

(47) Coulson, C. A.; Rushbrooke, G. S. *Proc. R. Soc. Edinburgh, Sect. A* **1948**, *62*, 350.

(48) (a) Fisher, M. E. *Phys. Rev.* **1961**, *124*, 1664. (b) Kasteleyn, P. W. *J. Math. Phys.* **1963**, *4*, 287.

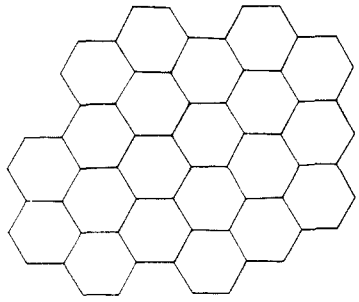

Figure 12. A 60-site benzenoid planar polyhex π-network with minimal periphery and relatively favorable resonance energy.

Each numbered criteria of section 1 failing to be met is indicated in parentheses; if it is a borderline failure, a question mark is appended; and if the cage is regular or semiregular this is indicated with a symbol r or s. As argued earlier we anticipate these numbered criteria to be important, while regularity and semiregularity are largely irrevelant.

11. Discussion

Numerous observations concerning the relative stability of various clusters are possible from the mass of data in Table III. We will attempt to organize the discussion by addressing the implications these data have for the various criteria enumerated in section 1.

Criterion 1: Three-Valent σ-Network. This is an a priori assumption in most of our present calculations, but it was earlier justified in that the other conceivable two- or four-valent structures would be substantially less stabilized for clusters of $v \gtrsim 30$. As a further partial test of this criterion for the $v = 60$ case we considered 60-atom fragments cut from the graphite lattice. The minimum number of dangling σ bonds is[49] 20 and the maximum number of disjoint Clar sextets (presumed[50,51] to be stabilizing) we found to be 8. Of about a half-dozen of these structures we treated, the most stable was found[52] to be that illustrated in Figure 12, as judged by the number (2786) of its Kekulē structures. The Kekulē-count resonance-energy estimate of 0.818 (graphite = 1.000), usually reliable for such benzenoid species, gives it less π stability than that for the uncorrected Buckminsterfullerene structure (number 32). Evidently this value is notably less than graphite because of the relatively great proportion of edges, restricting further delocalization of the spin-pairing patterns. With the curvature correction (i.e., π-interaction dimunition factor), the resonance energies of Buckminsterfullerene and of this graphitic fragment should be similar. But, of course, the comparative instability of this fragment is governed by the 20 dangling σ bonds, dominating strongly even over the σ-strain curvature correction for Buckminsterfullerene.

Criterion 2: Homeomorphic to a Sphere. Again this has been largely an a priori assumption in our present calculations. A partial test of the relevance of this criterion is made in the calculation on the planar graphitic fragment just mentioned. Especially for larger clusters the most favorable competitors of the simple cage structures are tori. Such tori, which unlike cages can be constructed without pentagonal rings, have a π-network equivalent to that of a graphitic fragment *with* cyclic boundary conditions, and thence presumably have a π-resonance energy per site comparable to that of (infinite) graphite, at least before curvature corrections are made. One of several 60-atom tori we tried has the unit cell of Figure 13 and was found[53] to yield a quite large

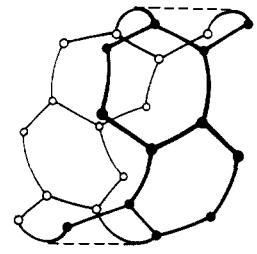

Figure 13. A unit cell which when iterated and joined in a cyclic manner yields a toroidal cluster.

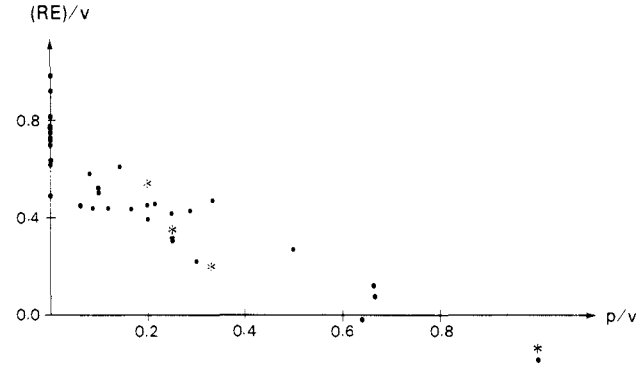

Figure 14. A plot of the resonance energy per site versus the ratio of the number p of abuttments between pentagonal faces to the number v of vertices. The points identify cages with only five- and six-membered rings, while the asterisks identify cages with two seven-membered rings each surrounded by five-membered rings.

Kekulē count of 41 297. Again for such a benzenoid the resultant uncorrected resonance energy per site relative to graphite, 1.097, should be reliable. Still, as noted earlier, the fact that curvature corrections for both resonant and nonresonant energies for tori are roughly twice those for spherical cages suggests that criterion 2 is appropriate, at least for smaller systems.

Criterion 3: Five- and Six-Sided Rings Only. In this case numerous calculations test this point. Various regular or semiregular polyhedra have three-, four-, eight-, and ten-sided faces, in which case they have notably smaller resonance energies than others like Buckminsterfullerene (cage 32). In addition, we have treated several polyhedra with a seven-fold symmetry axis, with two opposite seven-sided faces surrounded by five-sided faces. Such seven-sided rings adjacent to five-sided rings (as in azulene) might be expected to yield some stabilization since they allow the possibility of (stabilizing) 10 circuits around such a fused pair of rings. This expectation is indeed borne out by comparing the resonance energies for these heptagonal-symmetry polyhedra with the corresponding pentagonal-symmetry polyhedra that have the same unit cell. Yet the relative-resonance energy of none of these structures is very close to that of Buckminsterfullerene.

Criterion 4: Higher Symmetry. The species with greater resonance-energy stabilization for comparable values of v (namely, cages 24, 32, 39, 44, 49, 53, and 54) are all seen to have higher symmetries, with symmetry groups of order at least 20. Yet this criterion is tested only in part; the highest symmetry larger clusters also satisfy criterion 5. Thus it might be argued that criterion 5 is the one which is truly relevant. One test of this question is the $v = 84$ cage 46 of Figure 9, for which a resonance energy somewhat less than that of Buckminsterfullerene is obtained. Other checks are obtained for several other polyhedra with

(49) (a) Dias, J. R. *J. Chem. Inf. Comput. Sci.* **1982**, *22*, 15. (b) Dias, J. R. *Acc. Chem. Res.* **1985**, *18*, 241.

(50) Clar, E. *The Aromatic Sextet*; Wiley: New York, 1972.

(51) Herndon, W. C.; Hosoya, H. *Tetrahedron* **1984**, *40*, 3987.

(52) Dias, J. R. (*Can. J. Chem.* **1984**, *62*, 2915) gives a supposedly complete list of C_{60} graphite fragments, which, however, does not include that of Figure 12. In fact, there appear to be several missing fragments (all "grown" from Dias' nonradicaloid "cores").

(53) This is the maximum of those we tried that correspond to a more-or-less square section of graphite with cyclic boundary conditions. In fact, it appears that at fixed surface area (or number of sites) as a toroidal graph becomes skinnier (i.e., more like a bicycle tube) the Kekulē count per site increases upward from that for graphite. For the extreme over-strained case with a unit cell just one hexagon around a 60-site toroid, we find a phenomenal Kekulē count of 1 860 500. The type of unit cell of Figure 13 was chosen so as to make the curvature more nearly isotropic, as is desirable to minimize σ-strain.

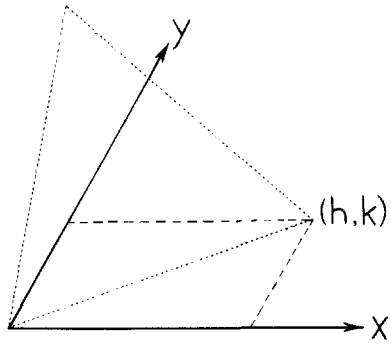

Figure 15. The choice of a triangular unit cell, identified by dotted lines, in terms of its positioning on a triangular lattice.

"marginal" symmetry, here interpreted to mean polyhedra with symmetry groups with orders in the range from 8 to 12. None of these cases yield a very high resonance energy.

Criterion 5: No Abutting Five-Sided Rings. There are numerous instances testing this criterion. In Figure 14 we plot the conjugated-circuit resonance energy per site versus the ratio of the number p of abutments between pairs of pentagons to the number of vertices v. All the structures made solely from five- and six-sided rings are included here, as well as those with two axial seven-membered rings that are adjacent to groups of five-membered rings. It is seen that there is a rough correlation as anticipated. That the special-marked points for seven-fold symmetric polyhedra are consistent with the general trend supports our rationale for the inclusion of these species.

Criterion 6: Uniform Curvature. This criterion was motivated in section 4 from a consideration of σ-strain, but it is strengthened by the π resonance energies. That is, cages with anisotropic curvature tend to have less resonance-energy stabilization. This is seen for the rather cigar-shaped polyhedra 23, 28, 29, 36, 38, and 47, with the long skinny unit cells in Figure 7. There is a sole exception to this: cage 44 with unit cell 71, for which the large central mass of hexagons evidently overcomes the effect of fusion of the five-membered rings. The π resonance energy in this case is not extremely high, and the cage thence probably is not extremely stable, because of the additional σ-strain due to anisotropic curvature.

Regularity and Semiregularity. Though this was not suggested here as a criterion relevant for chemical stability, it is implicit in some previous works on such structures. Still it is of some relevance to the extent that it tends to imply criteria 4 and 6, and, of course, the Buckminsterfullerene structure is semiregular. A "complete" test of the relevance of regularity or semiregularity was carried out with calculations on all such polyhedra with three-valent vertices. In addition to about a dozen such polyhedra in Table III, there is the infinite class of regular prisms. But for those prisms not included in the table, analytic results are available. The results (9.8) and (9.9) yield resonance-theoretic quantities, with an asymptotic resonance energy per site of

$$\frac{RE}{v} \to \frac{5-\sqrt{5}}{10}\left\{Q_1 + \frac{\sqrt{5}-1}{2}R_1 + \left(\frac{\sqrt{5}-1}{2}\right)^2 Q_2 + \left(\frac{\sqrt{5}-1}{2}\right)^3 R_2\right\} \quad (11.1)$$

The Hückel-MO model is also analytically soluble, with two bands

$$\epsilon^{\pm} = (2\cos(k) \pm 1)\beta \quad (11.2)$$

and yields an asymptotic resonance energy per site of

$$\frac{RE}{v} \to \left(\frac{\sqrt{3}}{\pi} + \frac{1}{6} - A\right)\beta \quad (11.3)$$

where A is the parameter discussed in section 8. In either case the resonance energy is destabilizing. In general the resonance energies of the regular and semiregular species are seen to be quite

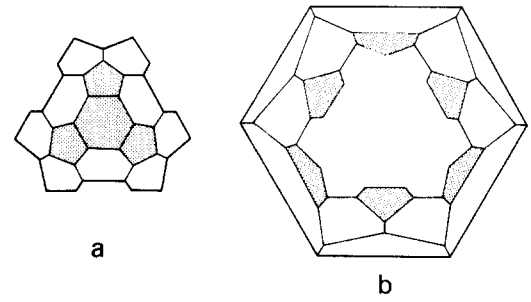

Figure 16. Growth of the Schlegel diagram for the smallest preferred class polyhedron with no abutting five-membered rings.

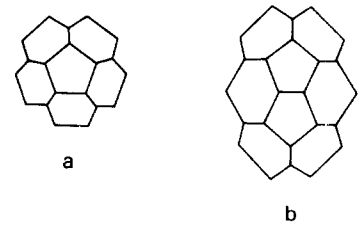

Figure 17. The structure for a single "isolated" pentagon (a), and for an "isolated" pair of pentagons (b).

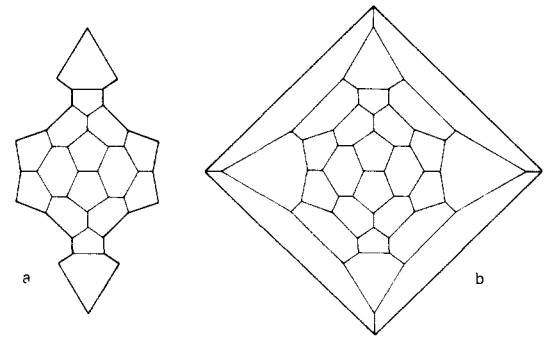

Figure 18. Attempt to grow a Schlegel diagram for a 48-vertex preferred class polyhedron with only "isolated" pairs of pentagons.

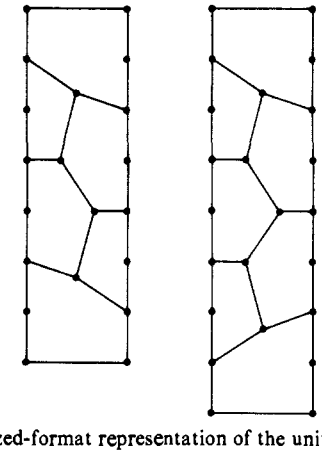

Figure 19. Stylized-format representation of the unit cells of Figure 6.

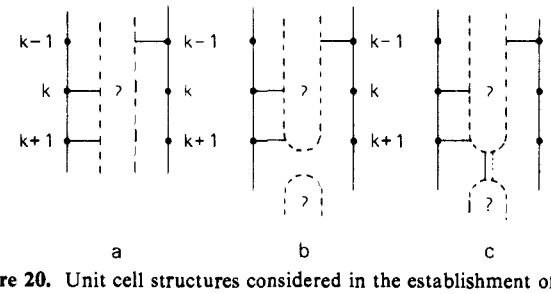

Figure 20. Unit cell structures considered in the establishment of rule R4.

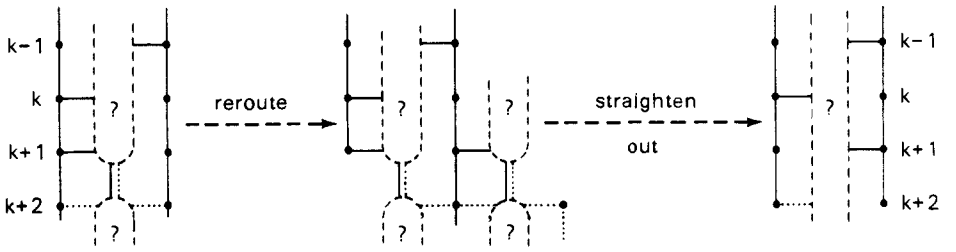

Figure 21. Unit cell transformation used in establishing rule R4. (The dotted lines indicate locations at which edge lines *might* occur.)

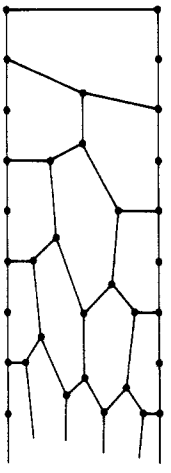

Figure 22. Deterministic pattern for the growth of a canonical unit cell in the region before reaching a five-ring.

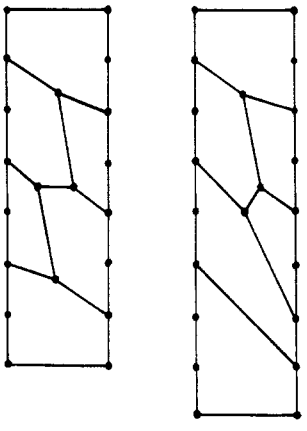

Figure 23. Two canonical unit cells which generate the same polyhedron.

small, with the exception of the C_{60} truncated icosahedron, which is the sole case satisfying all our preferred criteria. Little evidence is found for Haymet's suggestion[12] of special stability of the truncated icosadodecahedron C_{120} species.

12. Conclusion

Several results are reached in the present investigation:

(a) Criteria for stability of carbon clusters are developed and tested.

(b) σ-Strain effects are treated in a general manner and incorporated into the criteria.

(c) Systematic schemes for identifying and constructing polyhedral cages in the preferred classes are developed and applied.

(d) π-Electron computations on an extensive list of over 50 polyhedra are made and reported.

(e) Various qualitative correlations with experiment are noted near the end of section 2, and are further supported by our calculations. The Buckminsterfullerene structure appears to be the best candidate for the C_{60} species, and suggestions for the structures of observed C_{70} and C_{50} species are made.

(f) A few additional candidates for especially stable cages are identified, in particular, C_{72} (#39), C_{84} (#49), C_{180} (#53), and C_{240} (#54).

Still numerous questions remain. Further calculations on some of the more interesting cages could be of interest. Most particularly, questions concerning the kinetics and mechanism of formation remain. Nevertheless, the ideas elucidated and tested here should provide a useful basis for a more complete view.

Acknowledgment. The authors acknowledge helpful discussions with Professor R. E. Smalley, R. F. Curl, H. W. Kroto, and the Rice University experimental group, with members of the Rugjer Boskovic Theoretical Chemistry group, and with numerous other researchers.

Appendix A: Characterization of "Preferred" Icosahedral Symmetry Polyhedra

Here we classify all possible polyhedra with three-valent vertices, five- and six-sided faces, and overall icosahedral symmetry. This is conveniently done in terms of the *dual* polyhedra, obtained from our polyhedra by placing a new (dual) vertex in the center of each face of the original polyhedron and joining these (dual) vertices by (dual) edges whenever these vertices lie in adjoining faces of the original polyhedron. These dual polyhedra remain of icosahedral symmetry and have only triangular faces, 12 vertices of degree 5, and the remaining vertices of degree 6. Moreover, we can view the dual polyhedra as being formed from cells, just as we viewed the other polyhedra in section 7. But now the cells are triangular and correspond to the 20 faces of an icosahedron. The (dual) degree-5 vertices then must be located at the corners of these cells (since upon adjoining 20 such cells in an icosahedral fashion these cell corners lie at the icosahedron apices through which pass the five-fold symmetry axes). Thence all the remaining vertices inside, or only on the edges of a cell, have degree 6, so that the cell may be viewed simply as a (possibly quite large) equilateral triangular portion of the triangular lattice. Any such portion with the apices lying at lattice sites may be seen to be admissable.

To designate the sought-after cellular portions, we consider a coordinate system on the triangular lattice such that, first, a lattice site lies at the origin; second, the x axis lies along the direction from the origin site to one of the six nearest-neighbor sites, taken to lie a unit distance away; and, third, the (nonorthogonal) y axis is taken to lie at 60° with respect to the x axis. Then any admissable cell may be oriented with one apex at the origin and its "bottom" edge in the $+x$, $+y$ sector as indicated in Figure 15. The coordinate values h, k at the end of this bottom edge are such that h and k are nonnegative integers, and the area of this triangular cell may be computed to be $(h^2 + hk + k^2)\sqrt{3}/4$. But the triangular lattice's smallest (unit) cells, which turn out to be the faces of the dual polyhedron, have an area of $\sqrt{3}/4$. Thus the number of faces per cell is $h^2 + hk + k^2$, and the total number of faces on the dual polyhedron (composed from 20 such like cells) is the number given in eq 3.7, this also being the number of vertices of the corresponding original polyhedron. This result is evidently that of Caspar and Klug[54] though their proof seems to be unpublished.

Finally there is a question concerning the range of the h and k values. We may always choose h positive. Also, the interchange of h and k values leads to a mirror reflected cell, which is distinct from the original if $h \neq k \neq 0$. That is, the range for h and k

(54) Caspar, D. L. D.; Klug, A. *Cold Spring Harbor Symp. Quant. Biol.* **1962**, *27*, 1. See also: Goldberg, M. *Tohoku Math. J.* **1937**, *43*, 104.

to give different possible symmetry-inequivalent polyhedra is as indicated in eq 3.7. Further, the cage symmetries are those of the purely rotational icosahedral group I if $h \neq k \neq 0$, and I_h otherwise. Thence, all of the icosahedral-symmetry cages on which we carried out calculations have I_h symmetry except for the C_{140} cage, which has only I symmetry.

Appendix B: "Preferred" Polyhedra with Isolated Pentagons

Here we prove that the smallest three-valent convex polyhedron composed solely of pentagonal and hexagonal faces such that no two pentagons abut is *uniquely* the truncated (regular) icosahedron. From (3.8) we see that it must have at least $v \geq 60$ vertices, with equality occurring for the truncated icosahedron. Thus we need only show that there exists no other $v = 60$ polyhedron satisfying the hypothesis. Now (3.6) implies there are $f_6 = 20$ hexagonal faces, and (3.8) implies that no three of them may adjoin. Thus around any hexagon face there must be three pentagons as in the central shaded portion of Figure 16a. But further, around each of these pentagons there can only be hexagons, so that we "grow" the unshaded ring of hexagons in this same figure. Continuing yet further to avoid adjoining three hexagons at a point, one is led to add pentagons as at the shaded portions of Figure 16b, and then following this the unshaded hexagons around these pentagons. But what results is just the (Schlegel diagram) arrangement of faces on the surface of the truncated icosahedron.

Appendix C: Preferred Polyhedra without Adjoining Triples of Pentagons

Here we determine the smallest convex polyhedra composed solely of five- and six-membered rings such that no pentagonal face adjoins to more than one other pentagonal face. For such a polyhedron there then needs to be interspersed among the 12 pentagons a sufficient number of hexagons to so (partially) separate the pentagons. Around each isolated pentagon there are, as in Figure 17a, five hexagons each of which may be seen to adjoin to no more than three pentagons. Thence for each isolated pentagon there must be at least 5/3 hexagons. Around each abutting pair of pentagons there are, as in Figure 17b, six hexagons, two of which (adjoining to both pentagons) may adjoin with up to four pentagons, while the remaining four hexagons may adjoin to no more than three pentagons. Thence for each abutting pair of pentagons there must be at least $2/4 + 4/3$ hexagons. Thus letting p be the number of such abutting pairs of pentagons (and $12 - 2p$ the number of isolated pentagons), we obtain a lower bound for the number of hexagonal faces

$$f_6 \geq (12 - 2p)\frac{5}{3} + p\left(\frac{2}{4} + \frac{4}{3}\right) = 20 - p \qquad \text{(C.1)}$$

Then through the use of (3.6), a lower bound is obtained for the number of vertices for a polyhedron of the present class

$$v \geq 60 - 2p \qquad \text{(C.2)}$$

Then, in fact, $v \geq 48$, with the only possibility for equality in (C.2) occurring if $p = 6$.

These considerations lead us to consider the possibility of such a 48-vertex polyhedron (with $p = 6$). We attempt a construction starting with an adjoining pair of pentagons surrounded by hexagons, as in Figure 17b. To achieve equality in (C.2), the maximum number of pentagons adjacent to each of these hexagons must be realized, so that the placement of four additional pentagon pairs is dictated as in Figure 18a. But surrounding these pairs with hexagons leads to the structure of 18b, where now the outermost hexagons do not have the maximum number of adjoining pentagons and moreover the outer boundary is that of a (disallowed) quadrilateral face. Thus no such $v = 48$ polyhedron exists.

For $v = 50$ sites polyhedra of the present class with $p = 6$ or $p = 5$ arise as possibilities. An analysis of the same type as that of the preceding paragraph reveals exactly one such polyhedron for each of these choices of p. These two polyhedra are shown in Figure 3.

Appendix D: Sums over Discrete Curvature Measures

Under the circumstances[35] of equivalent hybrids to each of the three neighboring sites, the θ_i shown in Figure 4 are equal and the three bond angles ϕ_{ij} between the ith and jth associated σ-like bonds are equal. Also it may be shown[35b] that (in our notation)

$$2 \sin \phi/2 = \sqrt{3} \cos \theta \qquad \text{(D.1)}$$

Another angle of interest is a vertex's *defect* angle δ, that is, the amount by which a full (2π radian) rotation exceeds the sum of the bond angles at that vertex. Thence using a Taylor series expanded form of (D.1), one obtains

$$\delta \equiv 2\pi - (\phi_{12} + \phi_{23} + \phi_{31}) \simeq 3\sqrt{3}\,\theta^2 + O(\theta^4) \qquad \text{(D.2)}$$

(which up to the proportionality constant has been remarked upon before[16]). Further, without the assumption of equal θ_i or of equal ϕ_{ij}, it can be shown that corrections of no more than $O(\Delta\theta)^2$ and $O(\Delta\phi)^2$ appear.

Next we use the fundamental result

$$\sum_{\text{vertices}} \delta = 4\pi \qquad \text{(D.3)}$$

as was noted by Descartes[55] (ca. 1630) in an unpublished lost manuscript, for which handwritten notes made by W. G. Leibniz in 1676 have survived, long going unnoticed but finally published in 1860. Combining (D.2) and (D.3) we obtain the desired result (4.1).

Appendix E: Bond and Angle-Bending Energies

A brief discussion of the computations for Figure 5 is appropriate. The results for chains and (single) cycles were taken from Strickler and Pitzer.[24] The remaining cases were treated within a simple additive approach wherein the total energy, excluding π resonance, is given by

$$E = E^0 + E_{\text{np}}(\text{strain}) + E_{\text{ba}}(\text{strain}) \qquad \text{(E.1)}$$

Here E^0 is just a sum of bond energies, $E_{\text{np}}(\text{strain})$ is a strain energy due to any nonplanar distortions, and $E_{\text{ba}}(\text{strain})$ is a strain energy due to bond-angle bending away from the sp^2 ideal. Following Dewar and deLlano[56] for the bonds about an sp^2 center, each single bond has an energy of 4.3499 eV, and the nonresonant contribution of each double bond is 5.5378 eV. Thence, for the cages, tori, and graphite fragments E^0 is simply the appropriate sum over these values. For the graphite fragments the minimum perimeter and associated bond counts are taken from Dias' "periodic table" of benzenoids.[49]

For the cages and tori, the (surface) curvature strain is estimated, following Cyvin,[57] as

$$E_{\text{np}}(\text{strain}) = \sum \tfrac{1}{2}k(D\gamma)^2 \qquad \text{(E.2)}$$

Here the sum is over vertices, the force constant $k = 0.15$ mdyn/Å, the bond length is $D = 1.4$ Å, and

$$\gamma = (1/D)(-3z_0 + z_1 + z_2 + z_3) \qquad \text{(E.3)}$$

where z_0, z_1, z_2, and z_3 are the displacement coordinates of the vertices, as in Figure 4, with the displacements being measured normal to the surface. Then with the implementation of the ideas of Appendix D, $\gamma = -3 \sin \theta$, and for small deflection angles θ, we obtain

$$E_{\text{np}}(\text{strain}) = \tfrac{9}{2}kD^2\sum\theta^2 \qquad \text{(E.4)}$$

Thence, for cages, we find

$$E_{\text{np}}(\text{strain}) = \tfrac{9}{2}kD^2(4\pi/3\sqrt{3}) = 19.97 \text{ eV} \qquad \text{(E.5)}$$

(55) See, e.g.: Federico, P. J. *Descartes on Polyhedra*; Springer-Verlag: Berlin, 1982.
(56) Dewar, M. J. S.; deLlano, C. *J. Am. Chem. Soc.* **1969**, *91*, 789.
(57) Cyvin, B. N.; Neerland, G.; Brunvol, J.; Cyvin, S. J. *Z. Naturforsch., Teil* **1980**, *35*, 731.

For tori a value twice as great is used, as noted in section 5. For the cages we make a second strain correction, such as occurs in Cyvin's[58] expansion for in-plane vibrations, for the deviation of bond angles from the sp^2 ideal. For the preferred polyhedra with 12 pentagons and 60 pentagonal bond angles at 108°, this contribution reduces to

$$E_{ba}(\text{strain}) = 60 \cdot \frac{1}{2} k' D^2 \left(\frac{2\pi}{3} - \frac{3\pi}{10} \right)^2 = 6.44 \text{ eV} \quad \text{(E.6)}$$

where the force constant[58] is $k' = 0.4$ mdyn/Å.

Finally for the diamond fragments, with sp^3 centers and single bonds of length 1.5444 Å, we used Dewar and deLlano's[56] bond energy of −3.6957 eV. But in as much as Dewar and deLlano's values predict diamond to be just slightly more stable than graphite, we first algebraically cancel as much as possible, using the relation

$$\epsilon_g = \epsilon_d - \Delta + \epsilon_{res} \quad \text{(E.7)}$$

with ϵ_d (supposedly equal to -2×3.6957 eV) the energy per site for graphite, ϵ_{res} our graphite resonance energy per site estimate of 0.168 eV, and $\Delta = 0.019$ eV the experimental difference[59] in enthalpy between graphite and diamond.

Appendix F: Unit Cells for Preferred Polyhedra with Five- or Sixfold Symmetries

Here our method of constructing unit cells for our preferred class of polyhedra with five- or six-fold symmetries is considered. The unit cells are conveniently viewed in a stylized format preserving (graph-theoretic) connections but not geometric shapes: every cell is presented in a rectangular form with exactly two sites (located one in each corner) at each end and some number of sites distributed along the side boundaries (where the cell has been cut away from its neighbor cells). These latter sites, termed *boundary* sites, are chosen to be equally spaced along the two boundaries. As examples, consider the two cells of Figure 6 which are then redrawn as in Figure 19, whence these cells are seen to involve six and seven boundary sites on each side. Such sites when attached by a bond to a site in the interior of a cell are said to be *interiorly connected.*

Now for economy of effort a unit-cell generation scheme should generate as few as possible cells for the same (or an equivalent) polyhedron while at the same time guaranteeing at least one unit cell for each possible polyhedron. If different cells for the same polyhedron are possibly generated, this duplication is to be detected. Such duplication is largely avoided with the specification of the following *canonical* rules for our stylized format unit cells.

(R1) A cell is to have equal numbers of boundary sites on the two sides.

(R2) Of any two boundary sites an equal distance from the (top) end exactly one is interiorly connected.

(R3) The boundary site nearest the top of the left side is interiorly connected.

(R4) In proceeding down the side of a cell the boundary sites alternate between being internally connected or not, until possibly at the last position (nearest the bottom end).

Before elaboration of the freedom left for the completion of a unit cell, let us prove that these specifications are not so severe as to miss any possible polyhedra of our preferred class. First every such symmetric polyhedron has at least one unit cell. If the unit cell's boundary cuts through a face on one side, then because of the cyclic symmetry there must be a complementary cut face on the other side of the cell, and by moving one of these corresponding portions of a face to the other side one obtains a new cell incorporating a whole face there. Thus there exist stylized-format unit cells composed solely of whole faces (except for the two which contain the major symmetry axis and which do not explicitly occur in our unit-cell drawings). The cyclic symmetry then imposes the rules R1 and R2. The specification R3 is, however, merely a choice that is allowed: for if a cell not satisfying rule R3 is in hand, then that obtained by reflection about a vertical line satisfies rule R3 and describes an equivalent (mirror-image) polyhedron. Rule R4 is less trivial, and that it is not overrestrictive is to be established in a recursive fashion. We assume a cell satisfying this alternation criterion for all sites from the top down to a level k whereupon the alternation fails; thence we seek a transformation to a new cell satisfying the criterion down to level $k + 1$. The type of assumed situation is shown in Figure 20a. This is further refined into the subcases of b and c in Figure 20. Here the pattern of connections in question-marked regions is unspecified, and the dashed (vertical) line in (c) indicates the possibility of other bonds between the two question-marked regions. The horizontal bond issuing at level $k + 1$ in Figure 20c might in some cases be the same as the (solid) central vertical bond there. First we consider subcase (b) with special attention being given to the ring containing the sites on the left at levels $k + 1$ and $k + 2$. Evidently this ring must also contain sites on the right at levels $k - 1$, k, $k + 1$, and $k + 2$. In order to have no more than the six sites already on the ring, there would need to be a single bond connecting the two sites at level $k + 2$. But, because of rule R2, this could only happen if level $k + 2$ were at the bottom end of the cell. Thence nonalternation of the interior bonding can occur as in Figure 20b, but there only if the level $k + 1$ boundary sites are adjacent to the bottom end (as is permitted in rule R4). Next we consider Figure 20c, whence we transform to a new unit cell by selecting a new boundary leading from the level $(k + 1)$ site on the left into the interior (of the old cell) and avoiding the level $(k + 2)$ site on the left (in the old cell). This transformation, as indicated in Figure 21, incorporates a portion of the old unit cell on the right into the new one. Thus with repetition of these ideas, rule R4 is established.

With the rules Ri in place we now explore the remaining freedom for construction of unit cells. Much of this freedom concerns the placement of five-membered rings. From eq 3.5 we see that there are exactly two such five-rings per cell (neglecting, for fivefold symmetries, the two "undrawn" five-rings containing the major fivefold axis). It turns out that the remaining freedom apparently may simply be described as the choice of placement of these two five-rings. For instance, "growth" of a unit cell from the top end before encountering a five-ring is "deterministic". That is, there is but a single growth pattern, with the cell width (as measured by numbers of six-rings across) increasing with the level k, as indicated in Figure 22. After a single five-ring is encountered, growth is again deterministic with the cell width constant, and after the second five-ring is encountered, decreasing-width growth occurs down to the bottom end. Thence the two five-rings are (roughly) equal distances from the two ends of a cell. Once this distance is specified, some choice remains as to the horizontal positions of the five-rings. Thence all the canonical unit cells (say with up to six six-rings) are readily constructed.

There remains the question of whether any of the canonical cells (i.e., those satisfying rules Ri) might yield the same polyhedron. In fact, this does sometimes occur, as for the two cells of Figure 23. But still the duplication is limited as may be deduced on considering for a given polyhedron just what canonical cells are possible. First, there is a choice of a polyhedron or its (equivalent) mirror image, each of which might give different canonical cells. Second, after this choice one next seeks the five- and sixfold symmetry axis, which is unique except for the case of icosahedral symmetry whence any of the various fivefold axes are equivalent and must give rise to the same canonical cells. Third, given the axis one next chooses one end or the other as the "top" end of the cell; the two choices here might lead to different canonical cells. Fourth, one follows a path of bonds from the "top" end making alternant "right" and "left" turns except possibly at the last step before arriving at the "bottom" end. There are five or six choices for this path depending on which of the five or six vertices at the top end ring containing the symmetry axis are chosen as the starting point, but all are symmetry equivalent and do not lead to different canonical cells. Fifth, for the path from

(58) Bakke, A.; Cyvin, B. N.; Whitmer, J. C.; Cyvin, S. J.; Gustavsen, J. E.; Klaeboe, P. *Z. Naturforsch., A* **1979**, *34*, 579.

(59) Cox, J. D.; Pilcher, G. *Thermochemistry of Organic and Organometallic Compounds*; Academic: London, 1970.

the previous step, a $(2\pi/5$- or $(2\pi/6$-) cyclically related path is (uniquely) generated, and the pair of paths are taken as the boundaries of the canonical cell. The only ambiguity arising in this whole process involves a twofold choice for the chirality of the polyhedron and a twofold (orientational) choice for the "top" end of the cell. Thence there may be no more than $2 \times 2 = 4$ canonical unit cells for any polyhedron. This maximum number is divided by 2 if the polyhedron is achiral, and it is (further) divided by two if the polyhedron has a symmetry element interchanging "top" and "bottom" ends. Since the (frequent) presence of C_2 axes and/or reflection planes may ordinarily be readily ascertained from a cell, uniqueness is often readily determined. In the (apparently rather few) remaining cases the other cells associated to a given cell need be generated and checked against the (already complete) list of cells to identify the possibility of duplication. These equivalent canonical cells are conveniently generated by rotating the cell around so that ends and/or sides trade places, then "transforming" (as via processes in Figure 21) to obtain a canonical cell.

This overall scheme was applied to yield cells for distinct preferred-class polyhedra with $v \leq 88$. The results are as in Figures 6 and 7 and Table I. Finally, it is of some interest to note that the polyhedra of fivefold symmetry have v a multiple of 10, and those of sixfold symmetry have $v - 24$ a multiple of 12. This is seen from eq 3.6 if we note that the number of six-rings is a multiple of 5 for the case of a fivefold symmetry axis and, for the case of a sixfold symmetry axis, the excess of six-rings over the two containing the sixfold axis is a multiple of 6. These multiples of course are just the number of six-rings in a unit cell.

Registry No. Carbon, 7440-44-0; buckminsterfullerene, 99685-96-8; graphite, 7782-42-5; diamond, 7782-40-3.

How Is Transition State Looseness Related to the Reaction Barrier?

Sason S. Shaik

Contribution from the Department of Chemistry, Ben Gurion University of the Negev, Beer Sheva 84105, Israel. *Received November 10, 1986*

Abstract: Using a thermodynamic approach for the reaction class $Y + AX \rightarrow YA + X$, a link is drawn between barriers and transition state (TS) looseness. Thermochemical indexes are derived which allow the calculation of the thermochemical looseness of the TS from knowledge of the barriers for the forward and reverse directions ($\Delta E^{\ddagger}_f$, $\Delta E^{\ddagger}_r$). It is shown that high reaction barriers ($\Delta E^{\ddagger}_f + \Delta E^{\ddagger}_r$) are associated with thermochemically loose TSs. This correlation derives from two fundamental features of reactivity: (a) that high barriers are associated with TSs which are close to their dissociation limits, and (b) that reaction barriers derive from the deformations that are required to carry the ground-state molecules to the TS. The application is extended to solution-phase reactions, and an additional loosening effect emerges which accounts for the stability of the ions, $A^+ + X^-$. It is concluded that the thermochemical looseness involves bond distortion effects, which are dominated by the height of the barriers, and electron-density-depletion effects which are dominated by the stability of the ions. Computational and experimental data are discussed. Thermochemical looseness and geometric looseness correlate whenever bond stretchings are the main distortions which establish the TS. Thermochemical and geometric looseness will not correlate when bond stretchings are not the principal distortions which establish the TS. The lack of correlation between the two types of looseness may provide therefore, some information about the activation process. Potential application to other reactions is discussed.

The reaction rate is the direct and most rigorously defined reactivity observable. Associated with the rate is another experimental observable, the so-called reaction barrier. An elusive reactivity "observable" is the structure of the TS (transition state) which is a quest of physical organic chemistry. A fundamental question may then be posed, whether there exists any correlation between the measurable and the elusive reactivity "observables". For if such a relationship can indeed be established, it would then be possible to derive structural features of the TS directly from a measurement of reaction kinetics.

Such relationships have been previously deduced based on curve crossing principles in the context of the SCD model.[1-4] It has thus been shown that the TS of the identity S_N2 reaction (eq 1a)

$$X^- + CH_3X \rightarrow XCH_3 + X^- \qquad (1a)$$

becomes looser as the barrier increases.[1-4] A similar relationship was shown to carry over to nonidentity S_N2 reactions (eq 1b) where

$$Y^- + CH_3X \rightarrow YCH_3 + X^- \qquad (1b)$$

a correlation exists between the barrier in a certain direction (forward or reverse) and the looseness of the bond between the carbon and the leaving group.[4] How general is this relationship? Can it be shown to originate from principles which are not related to any particular modeling of the TS?

This paper applies a thermochemical approach[5] to deduce the relationship between barriers and TS structures for the archetype reaction class shown in:

$$Y + AX \underset{\Delta E^{\ddagger}_r}{\overset{\Delta E^{\ddagger}_f}{\rightleftharpoons}} YA + X \qquad (2)$$

Thermochemical indexes are derived, which allow the calculation of the TS looseness from knowledge of the barriers $\Delta E^{\ddagger}_f$ and $\Delta E^{\ddagger}_r$ in the gas phase and, with appropriate modifications, also in solution phase. The significance of the looseness indexes and of the relationship between the barrier and TS structure is discussed and shown to stem from the nature of the activation process. Potential applications to other reaction classes are discussed.

Theoretical Analysis

A. Gas-Phase Identity Reactions. The transition state for the gas-phase reaction in eq 2 possesses one coordinate which corresponds to loosening of the A-X and Y-A bonds. The energy

(1) Mitchell, D. J.; Schlegel, H. B.; Shaik, S. S.; Wolfe, S. *Can. J. Chem.* **1985**, *63*, 1642.
(2) Shaik, S. S. *Isr. J. Chem.* **1985**, *26*, 367.
(3) Shaik, S. S. *Can. J. Chem.* **1986**, *64*, 96.
(4) Shaik, S. S. *Prog. Phys. Org. Chem.* **1985**, *15*, 197 (pp 260-274).

(5) For previous mention of this approach see eq 42-44 in ref 4 (p 267), text footnote 1 in ref 3, and ref 2.

0002-7863/88/1510-1127$01.50/0